
High Performance Concrete in Washington State SR 18/SR 516 Overcrossing: Interim Report on Materials Tests

PUBLICATION NO. FHWA-RD-00-071

APRIL 2000



U.S. Department of Transportation

Federal Highway Administration

Research, Development, and Technology
Turner-Fairbank Highway Research Center
6300 Georgetown Pike
McLean, VA 22101-2296

FOREWORD

In the mid 1990's the FHWA established a High Performance Concrete (HPC) program aimed at demonstrating the positive effects of utilizing HPC in bridges. This, second of a two part interim report, presents preliminary test results from the first year of the materials testing program of the HPC mix used in the prestressed precast concrete girders on a bridge in the state of Washington.

This report is of interest to material engineers and bridge design engineers alike.

Copies may be obtained from the National Technical Information Service, 5285 Port Royal Road, Springfield, Virginia 22161.


T. Paul Teng, P.E.
Director, Office of Infrastructure R&D

1. Report No.	2. Government Accession No.	3. Recipient's Catalog No.	
4. Title and Subtitle High Performance Concrete in Washington State SR 18/SR 516 Overcrossing: Interim Report on Materials Tests		5. Report Date	
		6. Performing Organization Code	
7. Author(s) E. Fekete, P. Barr, J. Stanton, M. Eberhard, D. Janssen		8. Performing Organization Report No.	
9. Performing Organization Name and Address Washington State Department of Transportation, Olympia, WA 98504-7340 & University of Washington, 1107 N.E. 45 th St., Suite 535 Seattle, Washington 98105-4631		10. Work Unit No. (TRAVIS)	
		11. Contract or Grant No. DTFH71-96-TE036-WA-28	
12. Sponsoring Agency Name and Address Federal Highway Administration 6300 Georgetown Pike McLean, VA 22101-2296		13. Type of Report and Period Covered Interim Report January 1996 - November 1998	
		14. Sponsoring Agency Code	
15. Supplementary Notes FHWA contacts: Sheila Rimal Duwadi, Office of Infrastructure, R&D Terry Halkyard, Office of Infrastructure Barry Brecto, Washington State Division Office			
16. Abstract In the mid 1990's the FHWA established a High Performance Concrete (HPC) program aimed at demonstrating the positive effects of utilizing HPC in bridges. Research on the benefits of using high performance concrete for bridges has shown a number of benefits. These include increased span capacities, or wider girder spacings (and hence a fewer number of girders); increased concrete compressive and flexural capacities; and improved concrete durability. However, inspite all of these positive research results, relatively little has been done regarding the implementation of high performance concrete in bridges in the United States. The general goals of the FHWA program are: to encourage the States to implement HPC in bridges; to develop appropriate mix designs and establish quality control procedures; to encourage the use of larger diameter (15mm (0.6")) prestressing strands in the girders; to evaluate the performance of the structure; and to provide for technology transfer through development of a workshop (showcase). This report presents preliminary test results from the first year of the materials testing program of the HPC mix used in the prestressed precast concrete girders on a bridge in the state of Washington. State Route 516 utilizes WSDOT 74G pretensioned I-girders with a 190 mm cast-in-place composite deck. The girders were fabricated with 15mm diameter prestressing strands at 50 mm spacing, and designed for a concrete compressive strength of 69 MPa at 56 days. The material testing program includes determining compressive and tensile strengths, elastic modulus, long term creep, shrinkage, and thermal expansion properties of the HPC girder; and monitoring the compressive and tensile strengths, and elastic modulus variations of the deck concrete. This is the second of a two part interim report. The first report is titled, 'High Performance Concrete in Washington State SR18/SR516 Overcrossing: Interim Report on Girder Monitoring '.			
17. Key Word High Performance Concrete, bridges, mix design		18. Distribution Statement	
19. Security Classif. (of this report) Unclassified	20. Security Classif. (of this page) Unclassified	21. No. of Pages 74	22. Price

TABLE OF CONTENTS

SUMMARY	1
CHAPTER 1: INTRODUCTION	4
1.1: HPC IN PRETENSIONED BRIDGES	4
1.2: HPC IN WASHINGTON STATE BRIDGES	5
1.3: RESEARCH OBJECTIVES	6
1.4: SCOPE AND ORGANIZATION OF REPORT	7
CHAPTER 2: MATERIALS TESTING PROGRAM	8
2.1: OVERVIEW OF TESTING PROGRAM	8
2.2: SPECIMEN PREPARATION FOR CREEP TESTS	10
2.3: CREEP RIG DESIGN	14
2.4: CREEP TEST SCHEDULE	18
2.5: MONITORING OF CREEP RIGS	21
2.6: SHRINKAGE TESTS	22
2.7: FREEZE-THAW AND CHLORIDE PENETRATION TESTS	24
2.8: ABRASION RESISTANCE TEST	24
2.9: OTHER MATERIALS TESTS	24
CHAPTER 3: MATERIALS TESTS RESULTS	26
3.1: CREEP TESTS RESULTS	26
3.1.1: Total Strain	27
3.1.2: Components of Total Strain	33
3.1.3: Creep Strain	35
3.1.4: Creep Coefficient	40
3.1.5: Summary of Creep Test Results	43
3.2: SHRINKAGE TEST RESULTS	44
3.3: CONCRETE COMPRESSIVE STRENGTH	52

3.4: CONCRETE MODULUS OF ELASTICITY	54
3.5: CONCRETE TENSILE STRENGTH.....	55
3.6: CONCRETE COEFFICIENT OF THERMAL EXPANSION	56
3.7: DURABILITY.....	58
3.7.1: Freeze-Thaw Resistance.....	59
3.7.2: Chloride Ion Penetration	59
3.7.3: Chloride Penetration.....	59
CHAPTER 4: DISCUSSION OF RESULTS OF CREEP TESTS	60
4.1: MEASUREMENT RELIABILITY	60
4.2: SEALED AND UNSEALED CYLINDER STRAINS	62
4.2.1: Effect of Curing Conditions on Creep	62
4.2.2: Effect of Curing Conditions on Elastic Shortening.....	63
4.2.3: Effect of Basic Shrinkage.....	64
4.3: CREEP COEFFICIENTS.....	65
4.3.1: Unsealed Cylinders	65
4.3.2: Sealed Cylinders.....	67
4.4: VOLME-TO-SURFACE AREA RATIO.....	68
CHAPTER 5: PRELIMINARY CONCLUSIONS AND RECOMMENDATIONS	72
5.1: CONCLUSIONS	72
5.2: RECOMMENDATIONS FOR FURTHER RESEARCH	73
REFERENCES.....	74

SUMMARY

High performance concrete (HPC) is the name given to a class of materials that exhibits properties superior to those of conventional concrete. The superiority may lie in one or more of several attributes, such as strength, stiffness, freeze-thaw durability, or resistance to chemical attack. The properties are selected on the basis of the requirements of the particular application.

The Federal Highway Administration has recently developed a program to encourage the use of HPC in bridges. As part of this program, this project was undertaken to investigate the long-term behavior of an HPC pretensioned concrete girder bridge, with emphasis on the issue of prestress losses. This interim report provides preliminary results from the first year of the materials testing program. A companion interim report provides the preliminary results of the girder design, monitoring, and evaluation program.

The Washington State Department of Transportation (WSDOT) builds many precast, pretensioned concrete girders. In such bridges, the prestressing force decreases with time, because the steel relaxes, and the concrete undergoes elastic shortening, creep, and shrinkage. Accurate prediction of prestress losses, and thus the final prestressing force, is an important step in the design of any prestressed concrete girder bridge. To make this prediction, it is necessary to estimate the long-term creep and shrinkage properties of the concrete. An important goal of this study was to evaluate the long-term creep and shrinkage properties of a high-strength girder HPC mix used on the eastbound SR 516 overcrossing near Covington, WA..

The HPC mix was developed by the precast fabricator, Central Premix Prestress Co. of Spokane, WA. For the long girders, the precast fabricator was required to provide a concrete mix with a nominal strength of 51 MPa (7400 psi) at release of prestress and

69 MPa (10,000 psi) at 56 days. Although the shorter girders had less stringent strength requirements, they were cast using the same mix.

The materials testing program was conducted jointly by the fabricator, WSDOT and the University of Washington (UW). Central Premix monitored the compressive strength of match-cured cylinders as part of its quality control operation. Under contract with Central Premix, Wiss, Janney, Elstner Associates, Inc. (WJE) conducted freeze-thaw and chloride penetration tests on the girder HPC. The University of Washington is conducting a series of tests to determine compressive strength, tensile strength, elastic modulus, creep, shrinkage, and thermal expansion properties of the girder HPC. In nearly all cases, the concrete was taken from batches of material used in construction of the girders themselves. The cylinders for the creep and shrinkage tests were cast at the site, then transported back to the UW in Seattle for mounting in creep rigs.

A 6.1-m- (20-ft-) long test girder was cast in December 1996 in order to provide the fabricator with experience in handling the material. The test girder casting also provided the researchers with an opportunity to evaluate various specimen preparation procedures and to install instrumentation under field conditions. The bridge girders were cast during March and April of 1997. They were transported and erected in May 1997, and the deck was cast in September 1997. Because the time between the girder erection and deck casting was longer than had been scheduled, the researchers had the opportunity to take relatively long-term strain and deflection readings on the bare girders.

Six creep rigs, loaded with girder HPC cylinders, are being monitored. Measurements were taken: (1) on both 100 x 300 mm and 150 x 300 mm (4 in x12 in and 6 in x12 in) cylinders to investigate the effects of surface/volume ratio; (2) on sealed and unsealed cylinders; and (3) on cylinders stressed to 14, 21, and 28 MPa (2000, 3000, and 4000 psi) to study the effects of stress intensity. In all cases, companion cylinders were

left unstressed in order to evaluate shrinkage and to permit the creep strains to be computed from the values measured in the creep rigs.

UW researchers are also monitoring the compressive strength, tensile strength, and elastic modulus variation of the deck concrete. This concrete (designated as 4000D by WSDOT) has a required compressive strength of only 28 MPa (4000 psi), but it is expected to be more durable than conventional concrete. In addition, WSDOT is performing abrasion resistance tests on the deck concrete.

Considerable scatter was found in the creep and shrinkage test results. This scatter is largely attributed to the logistical difficulties of transporting the cylinders 300 miles from the casting yard in Spokane, preparing them, and loading them into rigs to be transported to Seattle under appropriate thermal conditions and according to a very tight time schedule. The result was that the maturity of the cylinders at the time of loading in the creep rigs varied in some cases from that of the girder concrete at release.

The HPC mix exceeded the WSDOT strength requirements, and performed extremely well during durability tests. In particular, WJE reported that: (1) the “coulomb” value was 1010 coulombs, (2) none of the samples tested exhibited any reduction in the dynamic modulus after 300 cycles of freeze and thaw, and (3) low chlorine permeability was measured during the long-term ponding tests.

At this time, the deck has been cast, but the results for the deck concrete materials tests are still being analyzed. Long-term materials tests and analyses of the girder HPC and the deck concrete will continue for approximately 2 years, as will the monitoring of the HPC bridge.

CHAPTER 1

INTRODUCTION

1.1 HPC IN PRETENSIONED BRIDGES

The Washington State Department of Transportation (WSDOT) frequently uses precast, prestressed concrete girders in its highway bridges. Such bridges are usually economical because they can be constructed for a low initial cost and they have proved to be durable in the Northwest. Judicious use of high performance concrete (HPC) offers the opportunity to further decrease the life-cycle cost of prestressed concrete bridges.

No unique definition of HPC exists, but two performance characteristics predominate: higher strength and improved durability. For a given girder cross-section, an increase in the concrete compressive strength makes it possible to prestress girders to higher levels of stress. This increased prestressing provides the designer with the options of increasing either the span length or the lateral spacing of the girders, ultimately reducing the number of girders and the total construction cost. HPC can also be used to increase the resistance to freeze-thaw cycles, increase abrasion resistance, and reduce chloride permeability. Each of these durability enhancements decreases maintenance costs and lengthens the service life of a bridge.

The enhanced performance characteristics of HPC are usually obtained by adding various cementitious materials and chemical admixtures to conventional concrete mix designs, and by modifying curing procedures. For example, the addition of fly ash and microsilica to concrete reduces the porosity of the concrete and increases its durability. Superplasticizers can be used to reduce the water-cement ratio and thereby increase the concrete compressive strength. However, even if the target properties are achieved, it is important to thoroughly test a new mix. Changes in mixes rarely affect only the target properties, in this case strength and durability, but they also affect other material properties, such as creep, shrinkage, modulus of elasticity, and coefficient of thermal expansion.

The creep, shrinkage, and stiffness properties of concrete strongly affect the prestressing losses in a prestressed girder. Most methods commonly used to calculate prestress losses have their roots in the 1970's when superplasticizers were unavailable, and the characteristics of concrete mixes differed from those used today. It is improbable that previously derived empirical methods will work well for HPC. For example, to achieve a high-performance concrete, it is often necessary to use a large percentage of cementitious materials. The corresponding increase in paste content may significantly affect the shrinkage and creep properties of the concrete. Research is needed to establish the long-term properties of HPC.

1.2 HPC IN WASHINGTON STATE BRIDGES

The WSDOT and the Federal Highway Administration (FHWA) recognized the need for research related to the calculation of the changes in prestressing forces. These agencies sponsored research, in part at the University of Washington (UW), to study these issues. FHWA is supporting related projects on HPC in Texas (Burns and Russell, 1996), Florida (Shahawy et al., 1992), and Tennessee (Deatherage and Burdette, 1994), among others.

The State Route 18 (SR 18) overpass over State Route 516 (RS 516) in Covington, 30 mi south of Seattle, was selected as a test project. The design of the bridge called for three spans, a short span at either end and one central long span (Figure 1.1). Each span consists of 5 girders, A - E, for a total of 15 girders. Each girder is identified by its span number and girder line (e.g., the long-span girder in the center of the bridge is identified as Girder 2C). The girders were standard WSDOT W74G girders. The girders were designed and built with high-strength HPC, and the deck was constructed with an HPC expected to exhibit good durability. The substructure was constructed using conventional concrete.

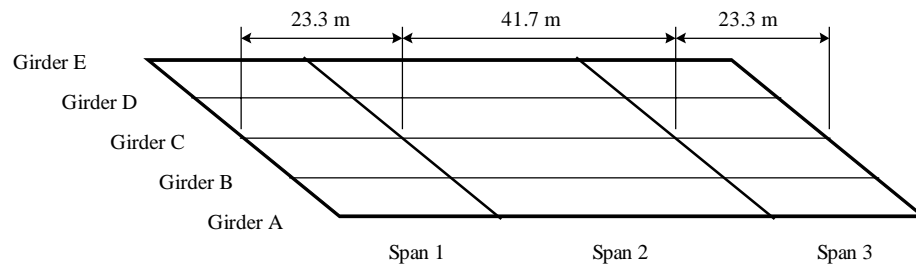


Figure 1.1. SR 18/516 Underpass

The bridge girders were cast at Central Premix Prestress Co. in Spokane, WA, using a mix developed by Central Premix. This bridge was the fabricator’s first experience with HPC girders, so a 6.1-m- (20-ft-) long Test Girder was cast to provide both the fabricator and researchers with experience with the new mix. The Test Girder also provided researchers with the opportunity to develop materials test protocols. The materials tests were particularly challenging, because the fabricator was located approximately 650 km from the UW materials laboratory in Seattle.

1.3 RESEARCH OBJECTIVES

The overall project focused on evaluating the effectiveness of using HPC in prestressed, precast concrete girders, with a focus on estimating prestress losses. As part of this project, it was necessary to establish the properties of the HPC used in the girder and deck. The objectives of the materials tests were as follows:

- Evaluate the creep, shrinkage, and thermal expansion properties of the HPC girder mix.
- Document the variation with time of the compressive strength, tensile strength, and elastic modulus of the HPC girder mix.
- Evaluate the durability properties of the HPC girder mix.
- Document the variation with time of the compressive strength, tensile strength, and elastic modulus of the HPC deck mix.

- Evaluate the durability properties of the HPC deck girder mix.

This report discusses the preliminary results of the girder concrete materials tests. The HPC deck mix results have not yet been analyzed.

1.4 SCOPE AND ORGANIZATION OF REPORT

This interim report provides the results from the first year of materials testing on the girder HPC. The end of the first year coincides approximately with the casting of the bridge deck. A companion report (Barr et al., 1998) discusses the design, evaluation, and monitoring of prestressed girders fabricated with the same HPC mix discussed in this report. This report is organized as follows:

- Chapter 2 describes the materials testing program, as well as the sampling, specimen preparation, and testing procedures.
- Chapter 3 presents the results of the material tests.
- Chapter 4 discusses the creep and shrinkage tests. Particular attention is paid to the reliability and significance of the measured material behavior.
- Chapter 5 presents the conclusions of the report.

CHAPTER 2

MATERIALS TESTING PROGRAM

2.1 OVERVIEW OF TESTING PROGRAM

The materials testing program for the high performance concrete (HPC) was undertaken to evaluate its strength, stiffness, creep, and shrinkage properties. The testing program, which is summarized in Table 2.1, included extensive testing on samples taken from three concrete batches. Materials testing began with specimens taken from the Test Girder, which was cast December 11, 1996. Subsequent testing used samples taken from one long bridge girder (Girder 2C, cast March 12, 1997) and one short girder (Girder 1C, cast April 2, 1997).

Table 2.1. Summary of Materials Tests

Time	Test Girder	Bridge Girders
Release	C E T	C E T
3 Days	C	C
7 Days	C E T	C E T
14 Days	C	C
28 Days	C E T	C E T
56 Days	C	C E T
Deck Casting		C
1 Year	C E	C E
2 Years	C E	C E
3 Years	C E	C E
Additional	TH FT CH	TH FT CH
Continuous	CR SH	CR SH
C - Compressive Strength TH - Thermal Expansion E - Elastic Modulus CR - Creep T - Tensile Strength FT - Freeze-Thaw CH - Chloride Permeability SH - Shrinkage		

These girders were selected for materials testing because they were instrumented to monitor long-term concrete strains (Barr et al., 1998). All tests were performed in the Materials Laboratory at the University of Washington (UW) and in the laboratory of Wiss, Janney, Elstner Associates, Inc. (WJE). The standard American Society for Testing Materials (ASTM) and American Association of State Highway and Transportation Officials (AASHTO) test procedures followed are listed in Table 2.2. The compressive strengths of 102 mm x 203 mm (4 in x 8 in) match-cured cylinders were also measured for all 15 girders by the fabricator.

Table 2.2. Testing Standards

Test	Specification	Laboratory
Compression Strength	AASHTO T 22	UW
Elastic Modulus	ASTM C 469	UW
Split-Cylinder Tensile Strength	ASTM C 469	UW
Creep	ASTM C 512	UW
Shrinkage	ASTM C 157	UW
Coefficient of Thermal Expansion	ASTM C 490	UW
Freeze-Thaw Resistance	AASHTO T 161	WJE
Chloride Ion Penetration (coulomb value)	AASHTO T 277	WJE
Chloride Penetration (1-year ponding)	AASHTO T 259 (modified)	WJE

Despite the various release strength requirements, the same mix design was used for the Test Girder and all production girders. The required release strength was 51 MPa (7400 psi) for the Test Girder and the long-span girders, and 35 MPa (5100 psi) for the short-span girders. All designs specified a 56-day compressive strength of 69 MPa (10000 psi). Table 2.3 summarizes the proportions for the mix design reported by the fabricator, Central Premix Prestress Co.

Table 2.3. Concrete Mix Proportions

Item	Type	Quantity	Abs. Vol (m³)	SSD Wt. (kg)
Coarse Aggregate	½ to #4, SG = 2.5		0.651	1203
Fine Aggregate	blended, SG = 2.3		0.228	525
Cement	Holnam Type III	429 kg	0.136	429
Fly Ash	Class C	131.0 kg	0.056	131
Silica Fume	MB Rheomac SF100	29.5 kg	0.013	29.5
Water		0.108 m ³	0.156	156
Air	entrapped	1%	0.01	0
Superplasticizer	MB Rheobuild 100			
WR Admixture	MBL 82			
Total			1.25	1827

2.2 SPECIMEN PREPARATION FOR CREEP TESTS

Test specimens were cast at the fabrication plant at the time the girders were cast. To perform standard ASTM and AASHTO tests, the researchers and WSDOT personnel cast numerous 152 mm x 304 mm (6 in x 12 in) cylinders and 76 mm x 102 mm x 406 mm (3 in x 4 in x 16 in) beams. To accommodate planned creep tests (Section 3.4), 102 mm x 304 mm (4 in x 12 in) cylinders were also cast. All cylinders were cast in oiled plastic molds. Oiled steel molds were used for the beams.

Several truck-loads of concrete were needed to cast each production girder. Two wheelbarrows of concrete were taken from one of the intermediate trucks for each of the girders to be sampled. The test girder required only slightly more than one truck-load of concrete, so only the first was sampled. All specimens were made using two lifts of concrete, one lift from each wheelbarrow, and were vibrated after each lift. Once all specimen molds were full and vibrated, the exposed ends were smoothed with a trowel. After the concrete had undergone its initial set, the final trowel finish was applied. Good quality finishes were needed for the creep tests.

After the girders had been cast and finished, they were covered with an insulating blanket and steam-cured. A thermocouple, attached to a prestressing strand and embedded in the girder, monitored the temperature history and controlled the application of steam in order to follow a pre-determined time-temperature curve. In practice, the heat of hydration was nearly sufficient to maintain the required temperature, so little steam was applied. Sure-cure cylinders were also linked to the thermocouple and were used by the fabricator to verify the release strength of the girder concrete.

The cylinders for testing at UW had to be transported from Spokane, WA, to the UW Materials Laboratory in Seattle for loading in the creep rigs. The two locations are separated by approximately 650 km (400 mi). The time needed to cure, transport, and prepare the cylinders for loading in the creep rigs precluded the possibility of match curing, if the creep rig loading was to take place at the same time as the girders were destressed. Instead, the cylinders were stored during transportation in insulated boxes that were designed to replicate in the cylinders the temperature history of the girders in their forms. To do so precisely was impossible, because the heat of hydration of the cement paste was the only heat source available. Trials with various insulation thicknesses led to the insulated box design shown in Figure 2.1. A thermocouple was used to monitor the temperature inside the box during transportation, which typically took about 6 h.

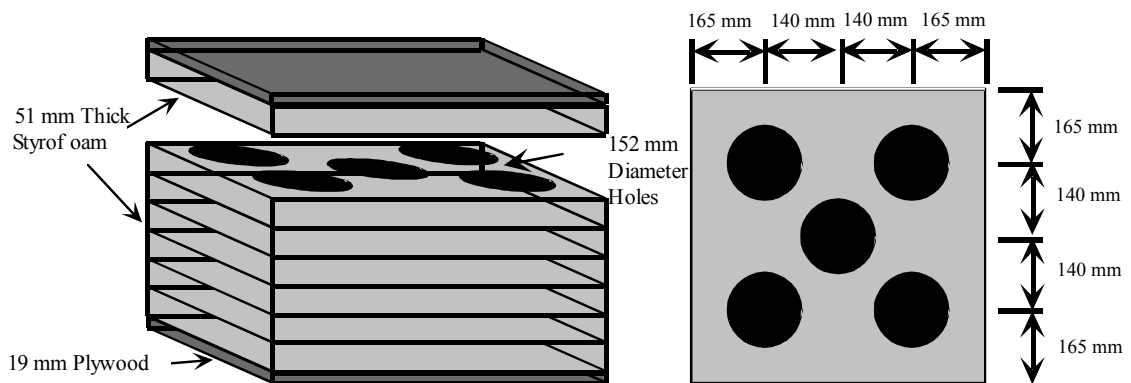


Figure 2.1. Insulated Boxes for Transportation and Curing of Cylinders

The insulated boxes were fabricated from several sheets of 51-mm- (2-in-) thick styrofoam attached to a plywood base with five 152-mm (6-in) diameter holes drilled for cylinders. Similarly constructed boxes were used for the beams, but because of the size and weight of the steel molds, only two beams were placed in each box. Once the specimens had been packed in the boxes, the lids were taped in place. The placement of the lid occurred approximately 2 h after casting for the Test Girder and Girder 1C specimens, but not until about 6 h after casting for the Girder 2C specimens, delaying the onset of the hydration process. Eight hours after casting, after the minimum time needed to avoid damage to the concrete during transportation, the boxes were loaded in a van and driven to the UW Materials Lab to prepare for loading in the creep rigs.

Once the cylinders arrived back at the UW, several preparation processes began. The specimens needed for early compressive strength tests were removed from the boxes and fitted with sulfur caps as needed. The shrinkage specimens were left in the insulated boxes until after the creep rigs were loaded, after which they were removed and gauge studs were attached to their sides with epoxy. At least two sets of gauge studs were attached on the sides of all Test Girder cylinders. Four sets were used on the specimens from both Girder 2C and Girder 1C. All sets of gauge studs were attached in pairs across diameters with a 254-mm (10-in) longitudinal separation. The two arrangements are shown in Figure 2.2.

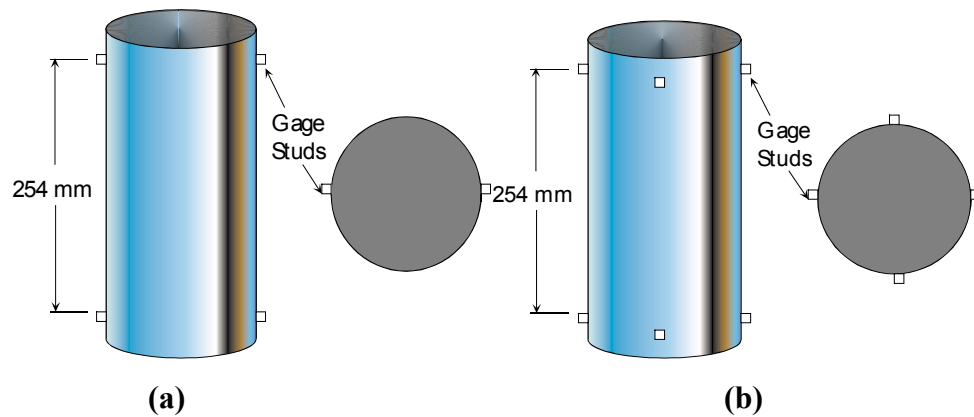


Figure 2.2. Gauge Stud Locations for (a) Test Girder and (b) Girders 1C and 2C

Two types of moisture boundary conditions were simulated: sealed and unsealed. To prepare the unsealed cylinders, the ends were smoothed and gauge studs were attached. To conserve time at this critical stage, the cylinders loaded in the creep rigs at the lowest stress level were fitted with sulfur caps. Specimens loaded to the higher stress levels were ground and flat and square to the cylinder's axis.

The sealed cylinders were coated over their curved surface with an epoxy to inhibit egress of moisture from the concrete. Then, the ends were smoothed and gauge studs were attached. All Test Girder specimens of this type had only two sets of studs, whereas four sets of studs were used on all specimens from the production girders (2C and 1C). It was crucial that these cylinders remain moist, so the Test Girder cylinders were placed in a hot water bath after being coated with the epoxy. However, the epoxy would not set in this moist environment, so the process was altered for the production girder cylinders. For the production girder cylinders, the specimens were allowed to sit in open air for approximately 1 to 2 h until the epoxy had set. This time in the open air decreased the temperature and, therefore, the rate of maturity gain of the concrete. To bring the cylinder back to the higher temperature, the cylinders were placed in an oven at approximately 54°C (130°F) once the epoxy had set. Approximately 1 h prior to loading the creep rigs, the specimens were submerged in water at room temperature to minimize thermal strains after loading.

2.3 CREEP RIG DESIGN

In prestressed concrete members, an important consequence of creep is that it leads to a substantial loss in prestress. To measure and quantify this effect, eight creep rigs were fabricated to apply a constant load to the specimens taken from the girder concrete. They were constructed in accordance with the creep test specifications of ASTM and are shown in Figure 2.3. The principle of the design is to apply a constant

load to a stack of cylinders between two steel plates by applying pressure with a pump beneath the lower plate and then locking in the load.

Five sets of two concentrically placed coil springs, supplied by Henry Miller Spring and Manufacturing Co. of Pittsburgh, PA, were added to each creep rig to maintain the load nearly constant as the specimens shortened. The springs had a maximum compression of 2 in, and an approximate stiffness of 2.35 kN/mm (13.4 k/in) for the spring with 203 mm (8 in) outside-diameter (O.D.) and 1.14 kN/mm (6.5 k/in) for the 117 mm (4⁵/₈ in) O.D. spring. Thus, the total stiffness of the five sets of springs was 17.5 kN/mm (100 k/in).

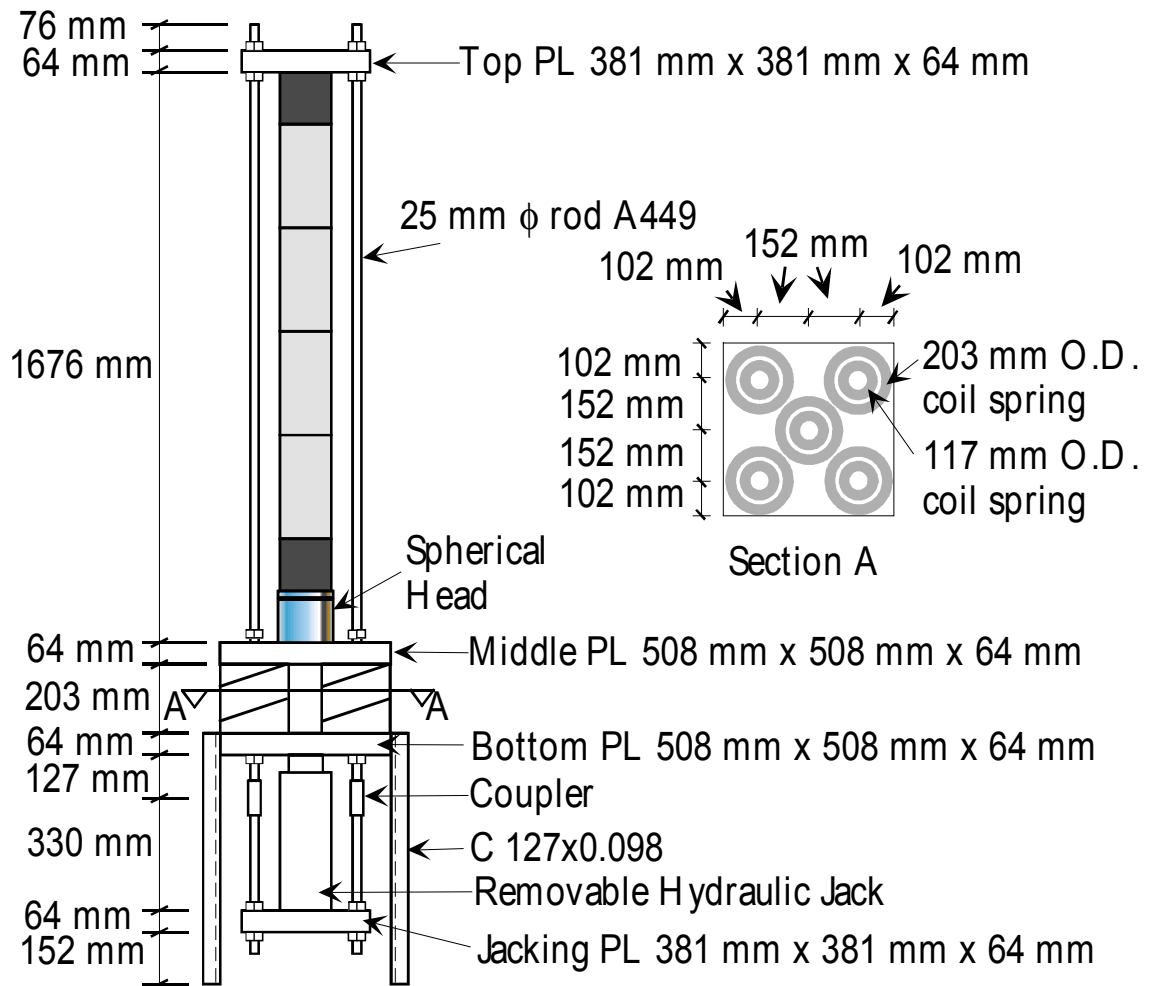


Figure 2.3. Creep Rig Design

The total stiffness of the four rods was approximately 175 kN/mm (1000 k/in), and that of the cylinders was approximately 420 kN/mm (2400 k/in), giving a ratio of specimen stiffness to creep rig stiffness of approximately 26. This ratio is high enough to minimize the load variation caused by cylinder shortening between readings. The spring properties limited the capacity of the creep rigs to 890 kN (200 kips). Difficulties in maintaining the rigs vertical and the load concentric in the first set of tests from the Test Girder concrete led to the installation of a spherical head in each creep rig before the next round of tests began on the Girder 2C cylinders.

The nuts on each side of the top plate are permanently fixed. They were tightened so that the connection between the rod and plate would restrain bending. The nuts below the bottom plate maintain the tension in the rods, and those above the middle plate are kept loose, with approximately 1.6 mm (1/16 in) clearance. Their purpose is to prevent the springs from extending in the event of unexpected cylinder failure.

A single 890-kN (200-kips) jack was used to stress the creep rigs. A trolley was fitted with an electric lift on which rested the jack, the jacking plate below it, and the short rods with couplers. To stress a creep rig, the trolley was wheeled under the rig, the lift was raised, the four short rods were connected to the rig rods using the couplers, the elevator was lowered, and the jack was loaded by a pump fitted with a pressure gauge. When the correct load was reached, the nuts below the bottom plate were tightened. The rig properties were such that each full turn of these nuts corresponded to a change in cylinder stress of

$$\Delta\sigma = \frac{pk_{\text{rig}}}{A_c} = \frac{3.20 \text{ mm} \times 15900 \frac{\text{N}}{\text{mm}}}{18200 \text{ mm}^2} = 2.77 \text{ MPa}$$

where p = pitch of the threads
 k_{rig} = combined stiffness of rods and springs
 A_c = cross-sectional area of a cylinder

The nuts could be tightened to an accuracy of about 1/10 of a turn, so the load on the most highly stressed cylinders, which were loaded to 27.6 MPa (4000 psi), is believed to be accurate to approximately ± 1 percent.

The creep rigs were loaded with either four 152 mm x 304 mm (6 in x 12 in) or two 102 mm x 304 mm (4 in x 12 in) cylinders, plus a half-length non-instrumented cylinder at each end of the stack. The end cylinders were used to minimize lateral confinement on the ends of the test cylinders. Half of the specimens in each rig were coated on their curved surfaces with epoxy, and the other half were exposed to air and allowed to dry. The sealed specimens were used to prevent the loss of moisture and simulate the behavior of a specimen with a large volume-to-surface ratio. These sealed and unsealed cylinders were stacked alternately in the creep rigs, and where they were not capped with sulfur, foil was placed at each end of the sealed cylinders to prevent moisture loss into the adjacent unsealed cylinder. A photograph of two creep rigs, one loaded with 152 mm x 304 mm (6 in x 12 in) cylinders and one with 102 mm x 304 mm (4 in x 12 in) cylinders, is shown in Figure 2.4.

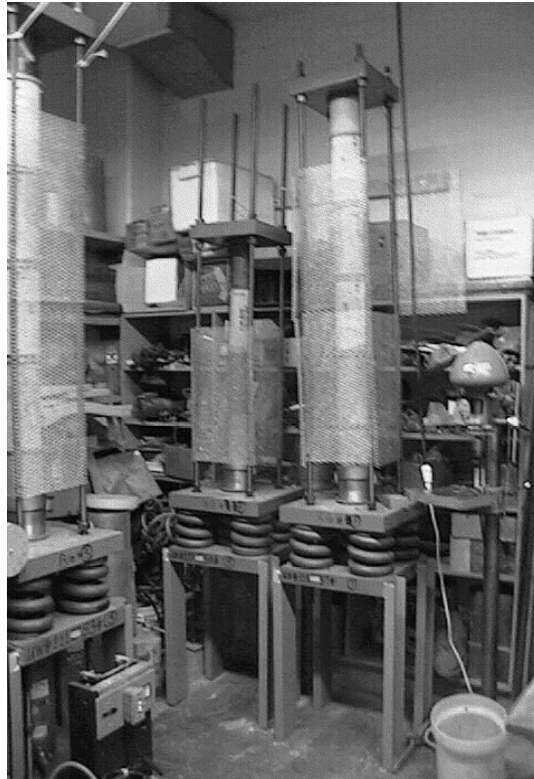


Figure 2.4. Photograph of Creep Rigs

2.4 CREEP TEST SCHEDULE

The contents of the eight creep rigs were changed several times during the course of the project. A creep test schedule is provided in Figure 2.5 for clarification. The purpose of the Test Girder materials test was to develop appropriate testing procedures.

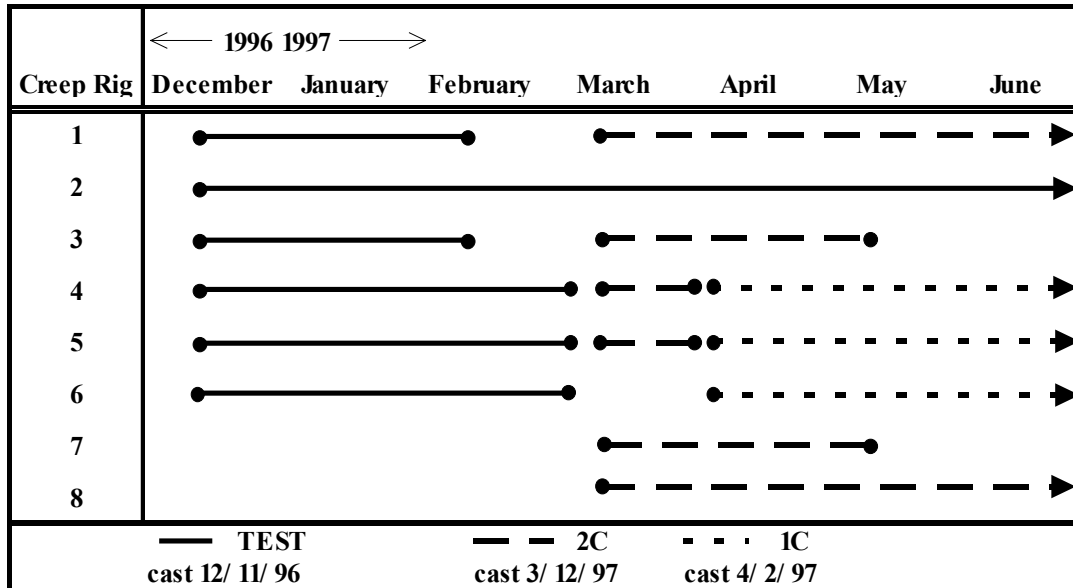


Figure 2.5. Time History of Creep Rigs

Initially, six creep rigs were loaded with specimens taken from the Test Girder (TEST) concrete and loaded as shown in Table 2.4. The Test Girder creep testing program was established to examine four variables: cylinder diameter (Rigs 1, 5, and 6), applied stress level (Rigs 1, 2, and 4), time of loading (Rigs 1 and 3), and drying versus sealed specimens. The strength and maturity gain in concrete is rapid in the first few days and the time of loading (or length of cure) was expected to significantly affect both the amount and rate of creep (Persson, 1997).

Table 2.4. Test Girder Loading Specifications

Rig Number	Cylinder Diameter (mm)	Stress Level (MPa)	Time of Loading
1	152	27.6	Release
2	152	20.7	Release
3	152	27.6	Delayed
4	152	10.3	Release
5	102	27.6	Release
6	102	27.6	Delayed

After several weeks of monitoring, it was determined that changes to the setup and procedure would greatly improve the quality of the data. Several lessons were learned from the Test Girder creep rigs. The epoxy on the sealed cylinders had in many cases failed to set and had caused the gauge studs to fall off. Also, in the absence of a spherical head, the load appeared to be applied at a significant eccentricity. Three measures were taken to eliminate these problems. The process of applying the epoxy and attaching the gauge studs was modified to ensure that they would not fall off. Four sets of gauge studs were used on all cylinders, so losing one stud no longer invalidated the data from an entire specimen. Furthermore, the diametrically opposing locations of the studs allowed for an accurate evaluation of the degree of eccentricity in the load. Compensation for the eccentricity in the load was made with the addition of the spherical head.

The opportunity to implement these changes arose with the casting of the long-span production girder (Girder 2C). The loading specifications for the new specimens are as listed in Table 2.5. All of the Test Girder cylinders, except those in Creep Rig 2, were removed. This rig was retained to provide the means of comparing the Test Girder concrete with the concrete in the production girders (2C and 1A).

Table 2.5. Girder 2C Loading Specifications

Rig Number	Cylinder Diameter (mm)	Stress Level (MPa)	Time of Loading
1	152	27.5	Release
3	152	20.7	Release
4	152	27.5	Release
5	152	27.5	Delayed
7	102	27.5	Release
8	102	27.5	Release

As shown in Table 2.6, three creep rigs were loaded with cylinders taken from the short-span production girder (Girder 1C). After several months of monitoring, it was necessary to free up two of the creep rigs (Rigs 3 and 7) for use on an unrelated project (Figure 2.5).

Table 2.6. Girder 1C Loading Specifications

Rig Number	Cylinder Diameter (mm)	Stress Level (MPa)	Time of Loading
4	152	20.7	Release
5	152	27.6	Release
6	152	13.8	Release

The long-term loading arrangement of the six remaining creep rigs is summarized in Table 2.7. The use of three different batches of concrete introduces a new variable. Although the mix design remained the same for each batch, the curing procedure varied, and changes were made to the equipment.

Table 2.7. Final Creep Rig Arrangement

Rig Number	Girder Sampled	Cylinder Diameter (mm)	Stress Level (MPa)	Time of Loading
1	2C	152	27.6	Release
2	TEST	152	20.7	Release
3	-	-	-	-
4	1C	152	20.7	Release
5	1C	152	27.6	Release
6	1C	152	13.8	Release
7	-	-	-	-
8	2C	102	27.6	Release

2.5 MONITORING OF CREEP RIGS

The strains were measured using a demountable, mechanical Whittemore (demec) strain gauge. This gauge consists of two pointed nodes approximately 254 mm (10 in) apart that are inserted in holes in the gauge studs on the sides of the specimens. The distances between the two nodes is recorded on a dial gauge that reads in increments of 0.003 mm (0.0001 in). Depending on the initial location of the gauge studs on the cylinder, it is possible to exceed the range of the gauge, 3 mm (0.1 in), and then it needs to be reset.

The reading process began with noting the date and time of the reading, as well as the ambient temperature in the testing room. The initial calibration measurement against a 254-mm- (10-in-) long mild steel rod was then recorded. Because of the location of the openings on the creep rig safety screens, the initial strain measurements were read for the “left” side sets of studs on all cylinders within one creep rig, and then all “right” sets were read. The first cycle of measurements was followed by a final calibration reading. The load was then reapplied to the rig using the jack and the sequence of initial calibration, strain measurements, and final calibration was repeated with the jack still in place. Before

Girder 2C casting, this procedure was appended to include a third cycle of readings taken after locking the load in and removing the jack. It was decided to take the readings after the release of the pump to guarantee that the amount of stress lost in the process of locking the nuts and in slippage of the nuts was minimal. These three cycles were then repeated for each creep rig.

The same reading cycle was used when the creep rigs were first loaded. The first cycle was an initial length measurement for all cylinders before they were loaded in the creep rig. The cylinders were then stacked inside the rig as they would remain throughout testing and the second cycle of readings, the first strain measurements, were taken. The load was then applied to the cylinders with the pump and a third cycle of readings was taken. The load was then locked in, and the pump was released. The final cycle of readings, except in the first few months of testing on the Test Girder cylinders, was then taken.

Measurements were made daily for the first week after loading. Subsequently, readings were taken weekly for 1 month, monthly for 3 months, and then every 3 months up to 1 year after loading. After 1 year, the frequency of readings will be changed to yearly.

2.6 SHRINKAGE TESTS

The test procedure used in this project differed from the ASTM standard. ASTM C157 requires that specimens be removed from their molds after 24 h and allowed to cure at 100 percent humidity for 6 days. Seven days after casting the first reading is taken, and the initial length of the specimen is determined. This procedure provides no information on the shrinkage occurring in the creep rigs during the first week, so it was altered. In this research, the companion shrinkage specimens were removed from their molds at the same time that the creep rigs were loaded, and they were kept in the same room. Readings were taken every time the creep rig strains were monitored.

Standard ASTM C157 shrinkage tests were performed using a concrete beam, [76 mm x 102 mm x 406 mm (3 in x 4 in x 16 in)]. There is a significant difference in the volume-to-surface ratio (V/S) ratio of the shrinkage beams and the cylinders used in the creep tests, so longitudinal shrinkage was also measured on cylinders of the same diameter as those in the creep rigs.

Much less preparation was required for shrinkage specimens than for creep cylinders. Once the specimens were removed from their molds, Whittemore gauge studs were attached to the sides of the cylinders 254 mm (10 in) apart in the same manner as the creep specimens, using epoxy. As with the creep specimens, only two sets of studs were used on those cylinders taken from the Test Girder and four on those cast from the production girders. This procedure differs from the one used in standard shrinkage beams. In standard tests the beams have the studs embedded in the ends, because they are read using a different apparatus.

For the samples taken from both of the production girders, several cylinder molds were modified to embed standard gauge studs in the ends of the specimens. A wooden disc was installed outside the cylinder mold at either end of the plastic molds to secure a gauge stud while the cylinder was cast. This strategy proved unsuccessful in the first attempt, but modifications made between the two production girder castings corrected the problems.

The same Whittemore gauge was used to monitor the strain in both the creep and shrinkage cylinders. A similar apparatus is used for the gauge studs at the ends of the cylinders, but it is not hand-held. The studs are rounded on their ends and the specimen is allowed to rest upright on one of the studs while a retractable node is placed firmly against the stud at the other end. The specimen is then rotated about an axis through the two studs, and the lowest reading is recorded. This tool also yields a least count of 10 microstrain.

2.7 FREEZE-THAW AND CHLORIDE PENETRATION TESTS

The specimen preparation for the freeze-thaw and chloride penetration tests are described by Sherman and Pfeifer (1998) in their WJE test report. According to the report, three 76 mm x 76 mm x 279 mm (3 in x 3 in x 11 in) concrete prisms were cast by Central Premix on December 11, 1996, for AASHTO T 161 testing. This date corresponds to the casting date for the Test Girder. Also, a single 102 mm x 204 mm (4 in x 8 in) cylinder was cast on December 3, 1996, for AASHTO T 277 testing. In addition, two 305 mm x 305 mm x 127 mm (12 in x 12 in x 5 in) slabs were cast in December 1996 for use in the modified AASHTO T 259 tests.

2.8 ABRASION RESISTANCE TEST

To be supplied by WSDOT.

2.9 OTHER MATERIALS TESTS

Compressive strength, elastic modulus, split-cylinder tensile strength, and coefficient of thermal expansion tests were conducted on the concrete from the Test Girder and both production girders.

The elastic modulus tests were performed using a mechanical extensometer. The cylinder was loaded to 50 percent of its measured compressive strength and the load-deflection diagram was plotted. The slope of this plot up to 40 percent of the compressive strength was used to calculate the modulus of elasticity. Later, a digital voltmeter was used in place of the plotter.

The coefficient of thermal expansion tests used 152-mm (6-in) diameter cylinders submerged in water. The temperature of the concrete was controlled by heating the water. The strains were measured for each given temperature, which ranged from 9°C to 40°C (48°F to 104°F).

CHAPTER 3

MATERIALS TESTS RESULTS

This chapter presents the results of the materials testing program. The most significant results of the creep tests are discussed in Chapter 4.

3.1 CREEP TESTS RESULTS

Creep is known to vary greatly with the moisture boundary conditions. Measurements from the sealed cylinders yielded basic creep (that which occurs in the absence of moisture egress), and those from the unsealed cylinders gave total creep. The drying creep was taken as the difference between them.

The measured creep strains were used to determine two different representations of creep. Specific creep is the total creep strain normalized by the level of applied stress and has units of microstrain/Pa. It takes into account only the stress applied to the concrete. The creep coefficient is a non-dimensional value that predicts the total creep strain as a multiple of the initial elastic strain. It accounts both for the level of stress applied and the modulus of elasticity of the concrete.

Only the results from those creep rigs monitored over the long term are presented here. Their loading specifications are provided in Table 3.1. The results from the other creep rigs can be found in Fekete (1997). The casting dates for the Test Girder (TEST) and the production girders (2C and 1C) are given in Chapter 2 (Figure 2.5).

Table 3.1. Creep Rig Loading Specifications

Rig Number	Girder Sampled	Cylinder Diameter (mm)	Stress Level (MPa)	Time of Loading
1	2C	152	27.6	Release
2	TEST	152	20.7	Release
3	-	-	-	-
4	1C	152	20.7	Release
5	1C	152	27.6	Release
6	1C	152	13.8	Release
7	-	-	-	-
8	2C	102	27.6	Release

3.1.1 Total Strain

Total strain is the sum of the elastic, creep, and shrinkage strains. The total strain in the sealed and unsealed specimens for the six creep rigs is reported in Figures 3.1 to 3.6. The plots show the strain in each cylinder and the average of like specimens in the creep rig. With the exception of three of the four specimens in Creep Rig 2, the line plotted for each cylinder is the average of four measurements. Plots showing the measurements from each pair of gauge studs on the specimen are provided in Fekete (1997). The “age” of the concrete in the plots is the time elapsed since casting. The length of time for which measurements are plotted depends on the time of casting of the specimens.

Table 3.2. Maximum Total Strains

Rig Number	Stress Level (MPa)	Cylinder Diameter (mm)	Unsealed Maximum	Sealed Maximum
1	27.6	152	-3430	-2670
2	20.7	152	-2400	-1680
4	20.7	152	-2620	-2510
5	27.6	152	-3280	-3970
6	13.8	152	-1840	-1620
8	27.6	102	-3790	-3790

Table 3.2 provides a summary of the maximum total strain for sealed and unsealed cylinders in all six creep rigs. As expected, the plots of total strain are characterized by a large initial strain followed by a gradual increase in strain with time. The differences in strains between nominally identical cylinders were relatively small. The average variation for identical cylinders lies within ± 3 percent of their average, except for the unsealed specimens in Creep Rig 1 (± 5 percent) and Creep Rig 6 (± 9 percent), and the sealed specimens in Creep Rig 2 (± 4 percent). There is only one specimen of each type in Creep Rig 8 (Fig. 3.6).

The total strain histories for Creep Rig 1 (Figure 3.1) show three distinct slopes between the ages of 42 and 105 days, 105 and 122 days, and thereafter. These differences result from an error in applying the load at an age of 42 days. The needle on the pressure gauge of the pump stuck, and the jack applied a concrete stress to the cylinder that exceeded the intended 27.6 MPa (4000 psi). The distinct change in slope at 42 days to a steeper negative slope until 105 days corresponds to the time that this higher load was maintained. The positive slope between 105 and 122 days represents the sum of creep

occurring under the reapplied 27.6 MPa (4000 psi), plus the elastic recovery of the strain from the higher load. The slope after 122 days is for the correct load of 27.6 MPa (4000 psi) after all recovery has occurred. It is less steep than that seen between 42 and 105 days.

The Test Girder was cast first, so the strain history for Creep Rig 2 (Figure 3.2) is the longest, extending to 300 days. The curve formed by this data is not as smooth as many of the others. This is, at least in part, due to the problem with the springs in the Whittemore gauge that were repaired after casting the Test Girder. Creep Rig 4 had little scatter and consistently increasing total deformation.

The relative magnitudes of the unsealed and sealed cylinders in Creep Rig 5, shown in Figure 3.4, are the reverse of those expected; the unsealed cylinders had less total strain than the sealed cylinders. The additional strain in the sealed specimens appears to have taken place in the first week after the load was applied. At application of the load, the sealed specimens had -1500 microstrain compared with only -1220 microstrain in the unsealed specimens, a difference of nearly 300 microstrain. Subsequent incremental strain measurements during the first 5 days were an average of 50 percent larger for the sealed than the unsealed cylinders, but only 20 percent by day 7. The concrete was obtained from the same batch. The reason for the differences is unknown.

The total strain histories for the specimens in Creep Rig 6 are shown in Figure 3.5. The unsealed specimens show more scatter than is seen in the sealed specimens

Figure 3.6 represents the long-term data for 102-mm (4-in) diameter cylinders (Creep Rig 8). The sealed and unsealed specimens experienced almost identical strains. This strain is higher than that observed in any specimen other than the sealed specimen in Creep Rig 5. The large strains in the unsealed cylinders can be attributed to a smaller volume-to-surface ratio that yields more shrinkage strain, but also to a difference in curing. The large strain in the sealed cylinders has not been explained.

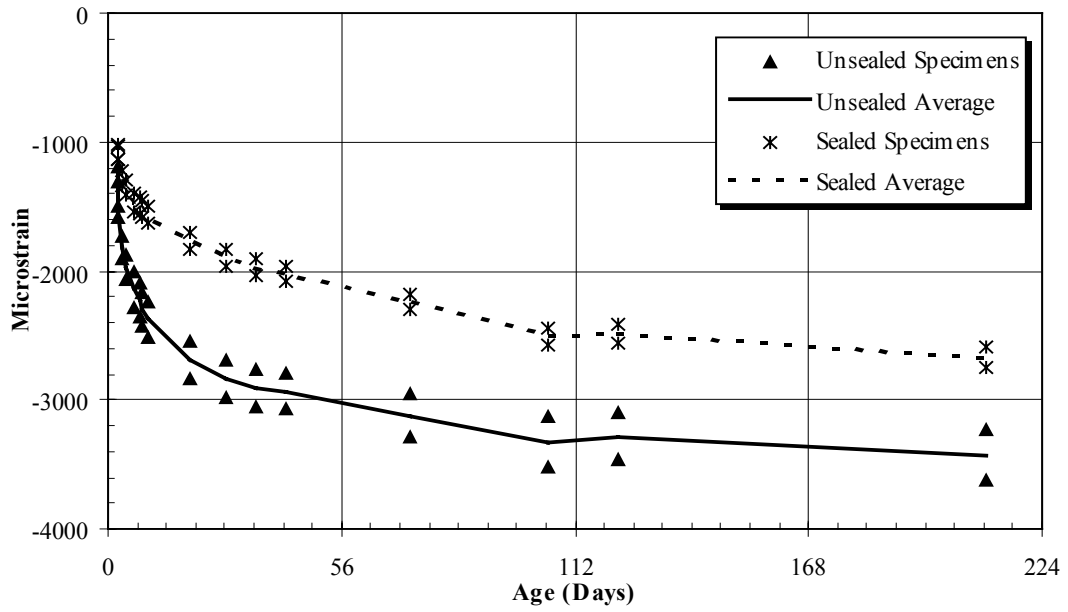


Figure 3.1. Creep Rig 1 Total Strain (152-mm Diameter, Girder 2C, 27.6 MPa)

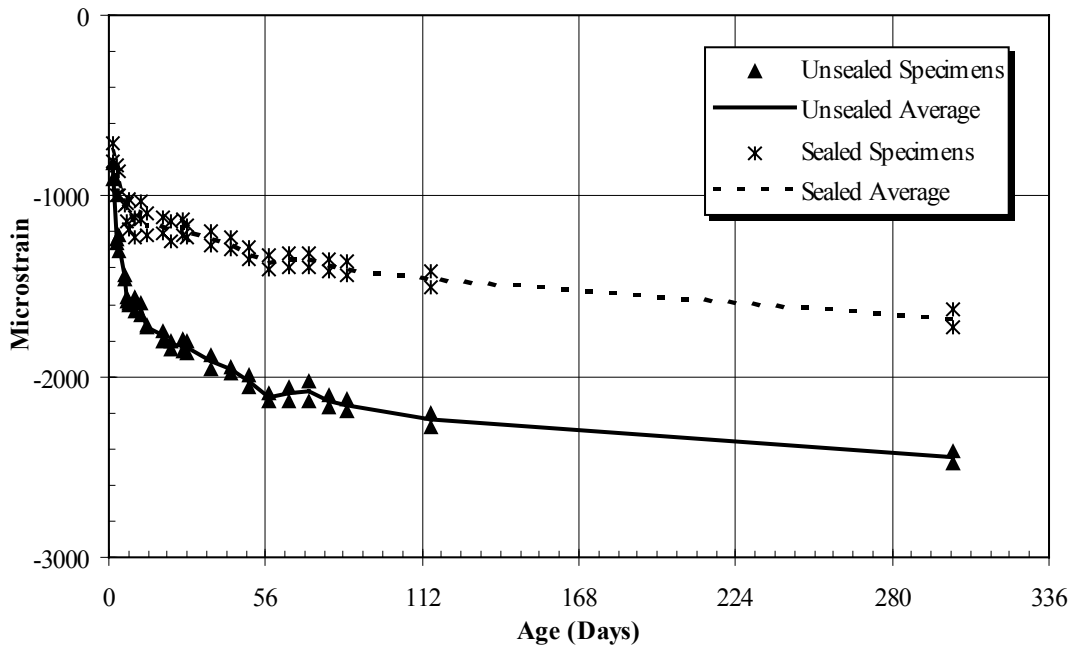


Figure 3.2. Creep Rig 2 Total Strain (152-mm Diameter, TEST, 20.7 MPa)

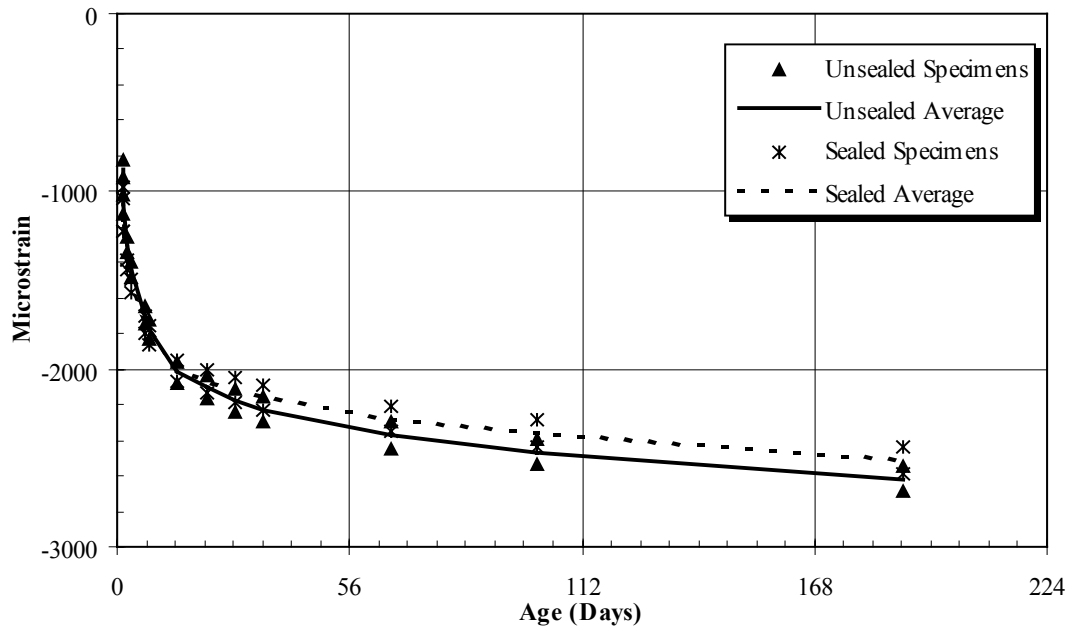


Figure 3.3. Creep Rig 4 Total Strain (152-mm Diameter, Girder 1C, 20.7 MPa)

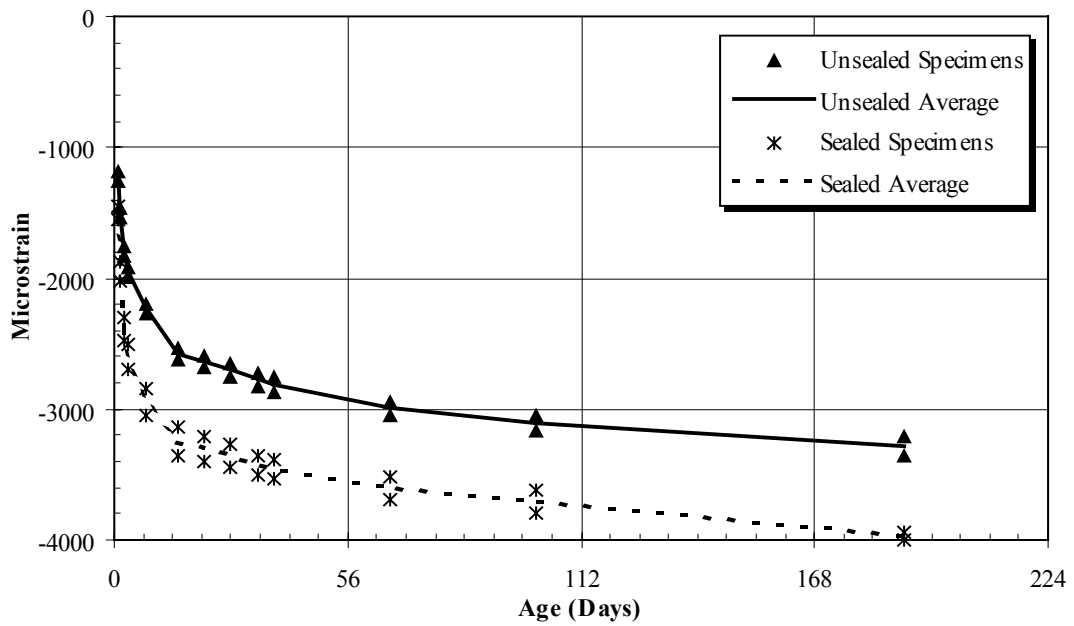


Figure 3.4. Creep Rig 5 Total Strain (152-mm Diameter, Girder 1C, 27.6 MPa)

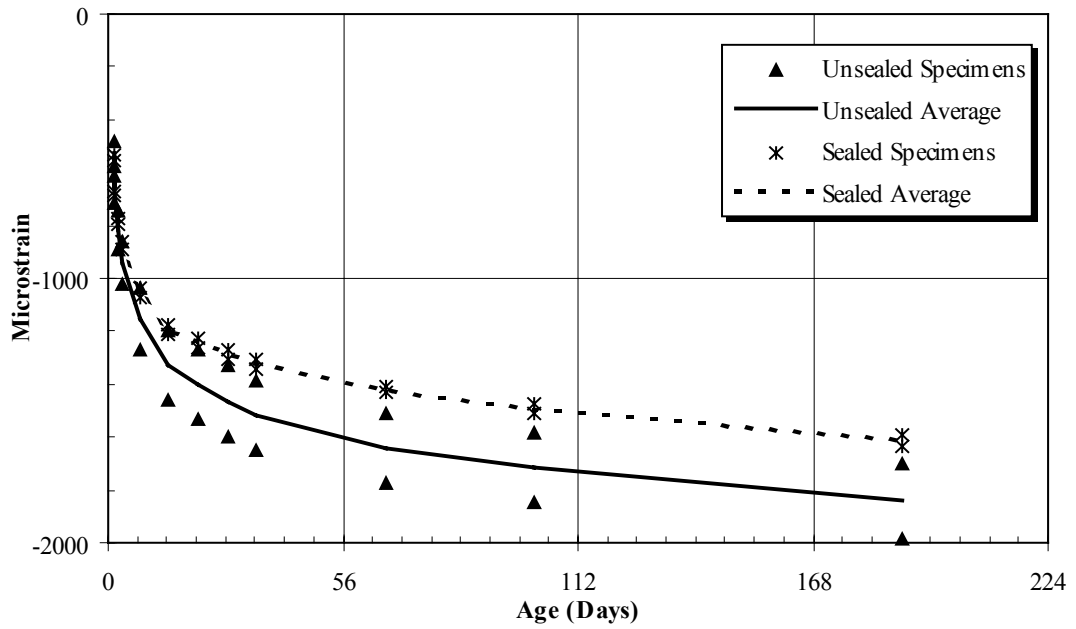


Figure 3.5. Creep Rig 6 Total Strain (152-mm Diameter, Girder 1C, 13.8 MPa)

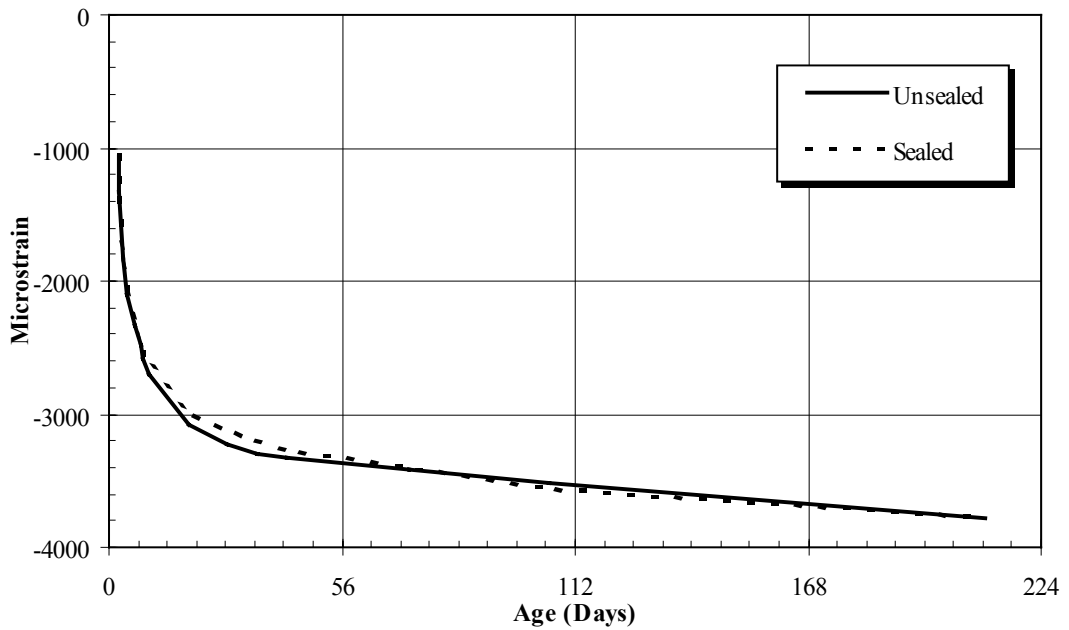


Figure 3.6. Creep Rig 8 Total Strain (102-mm Diameter, Girder 2C, 27.6 MPa)

3.1.2 Components of Total Strain

Using the total strains and the results of other materials tests, an analysis was conducted to separate creep into its components. The following is a summary of the analysis procedure.

- The elastic shortening was subtracted from the measured strains of all specimens to separate the time-dependent strains. Elastic shortening was calculated using the level of stress applied and the modulus of elasticity of the concrete at the time of loading. The testing for determining the modulus of elasticity is described in Section 3.5, but a summary, including the value of the initial elastic strain subtracted for each creep rig, is provided in Table 3.3.

Table 3.3. Initial Elastic Strains

Creep Rig	Applied Stress (ksi)	Elastic Modulus (GPa)	Initial Elastic Strain (microstrain)
1	27.6	33.2	-830
2	20.7	32.5	-640
4	20.7	28.3	-730
5	27.6	28.3	-980
6	13.8	28.3	-490
8	27.6	33.2	-830

- The shrinkage strain was subtracted from the total time-dependent strains of the unsealed creep specimens, yielding the total creep. The value subtracted was determined using a fitted curve [of the form $\epsilon_{sh} = A \ln(t)$] to the measured data of the companion unloaded cylinders. These curves are shown in Section 3.3. This procedure was followed to decrease the effect of random reading errors.

These calculations follow normal practice; however, they fail to address several issues. First, the modulus of elasticity increases over time, which, in the absence of creep, might be expected to cause an elastic lengthening in a cylinder under constant stress. The effect is not large, and arises from the conventional approach of modeling the behavior as an elastic component independent of time, and several time-dependent components.

Second, basic shrinkage was not measured. Basic shrinkage is often considered a secondary factor in concrete exposed to drying at an early age, usually only about 5 percent of the ultimate drying shrinkage (Bazant and Xi, 1994). However, for high strength concrete with a low water-cement ratio, it plays a much larger role in the early shrinkage (Han and Walraven, 1996). Also, the use of silica fume creates a finer pore structure that increases the basic shrinkage. Presumably, basic shrinkage existed in both the sealed and unsealed creep cylinders and in the (unsealed) shrinkage cylinders. Thus the basic and drying shrinkage strains were subtracted from the unsealed cylinders, leaving only the total creep strains. On the other hand, the data from the sealed cylinders, which is presented as basic creep, really consists of basic creep plus basic shrinkage that occurs after loading the rigs.

3.1.3 Creep Strain

The basic and total creep strains for the six creep rigs are shown in Figures 3.7 to 3.12. A summary of the maximum total and basic creep strain in each of the six creep rigs is provided in Table 3.4.

Table 3.4. Summary of Maximum Creep Strain

Rig Number	Stress Level (MPa)	Cylinder Diameter (mm)	Maximum Total Creep	Maximum Basic Creep
1	27.6	152	-2260	-1840
2	20.7	152	-1410	-1040
4	20.7	152	-1430	-1780
5	27.6	152	-1870	-2990
6	13.8	152	-800	-1130
8	27.6	102	-2840	-2960

The same trends are exhibited in these strain histories as are seen in the total strains for the six creep rigs (Figs. 3.1 to 3.6), except that, having subtracted the shrinkage strains from the unsealed specimens, the relative magnitudes have reversed in Creep Rigs 4 and 6 (Figures 3.9 and 3.11). As is the case in Creep Rigs 5 and 8 (Figures 3.10 and 3.12), the sealed specimens in Creep Rigs 4 and 6 (Figures 3.19 and 3.11) experienced basic creep strains in excess of the total creep strains in the unsealed specimens. It was anticipated that the total creep strains would exceed the basic creep strains, as is true in the cylinders of Creep Rigs 1 and 2, shown in Figures 3.7 and 3.8.

Several factors are believed to have contributed to these irregularities. The inclusion of the basic shrinkage component in the sealed cylinder results is one such factor. This factor does not appear to be the largest contributor, however, given that the difference between the basic and total creep values in Creep Rig 5 (Figure 3.11) is 1150 microstrain. Basic shrinkage values are usually less than 100 microstrain and reach 700 microstrain only in extreme cases (Neville, 1995).

The unsealed specimens in Creep Rigs 4 and 5 are exhibiting strains of similar magnitude to the unsealed specimens in Creep Rigs 2 and 1, at the same stress levels.

Therefore, it would appear that the discrepancy lies in the results of the sealed specimens. The fact that this irregularity occurred in all three of the Girder 1C creep rigs suggested that it was related to a difference in the concrete. The large discrepancy at an early age points to the curing process in particular. The most likely cause was a lower maturity, and therefore strength, at the time of loading due to the coating process.

To prepare the specimens, they were removed from the insulated boxes, and the high hydration temperature was not maintained. Although they were placed in an oven to return the temperature to that of the hydration, the unsealed cylinders never lost any heat. There was no time to ensure that the maturity of the sealed specimens was comparable to that of the unsealed specimens.

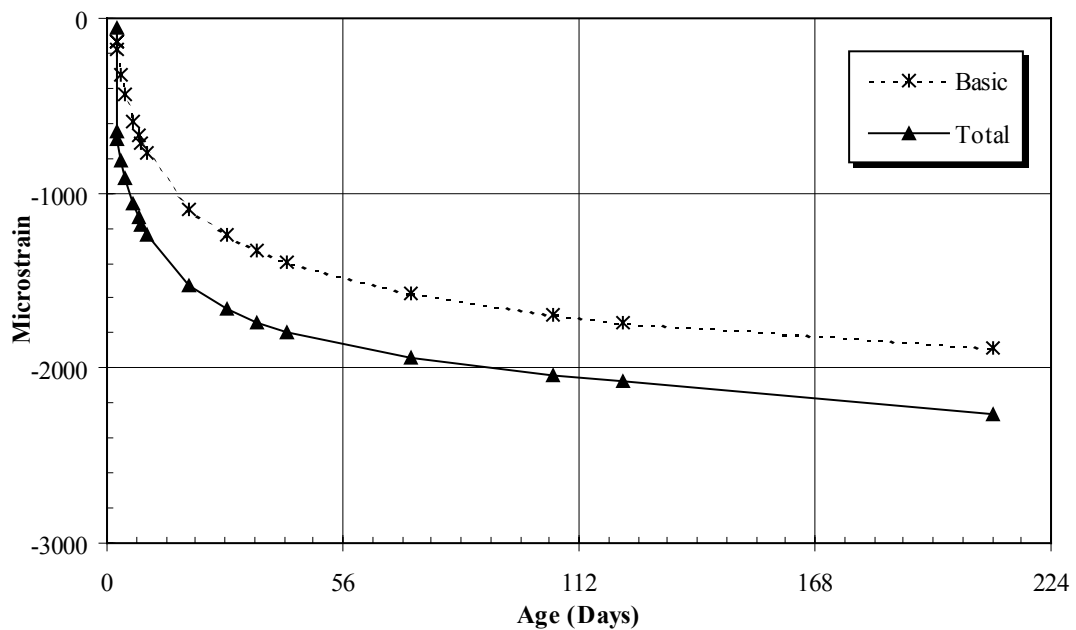


Figure 3.7. Creep Rig 1 Creep Strain (152-mm Diameter, Girder 2C, 27.6 MPa)

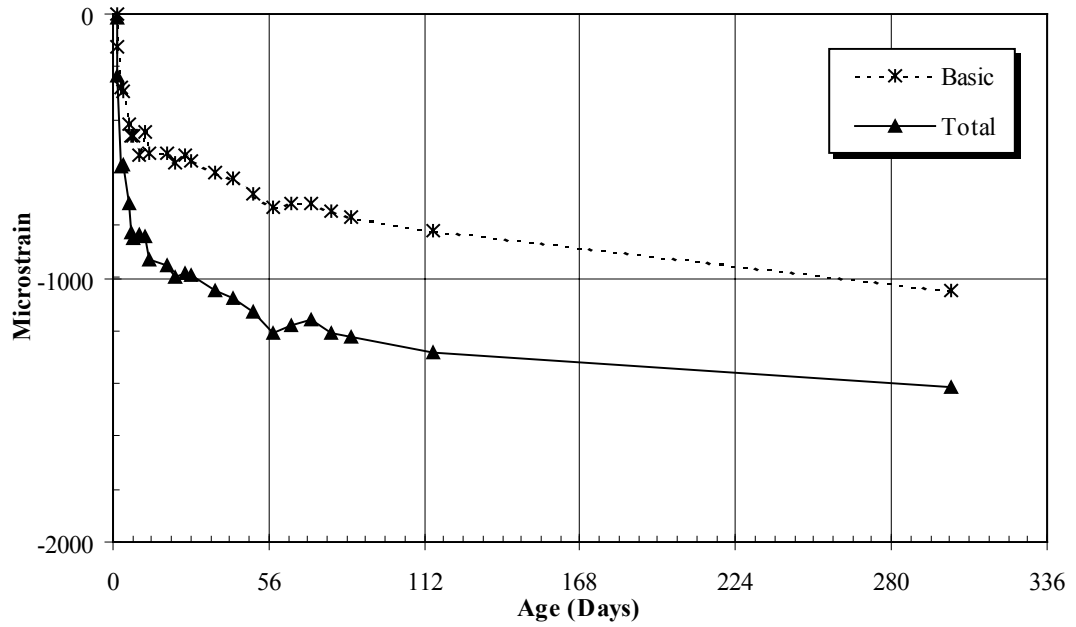


Figure 3.8. Creep Rig 2 Creep Strain (152-mm Diameter, TEST, 20.7 MPa)

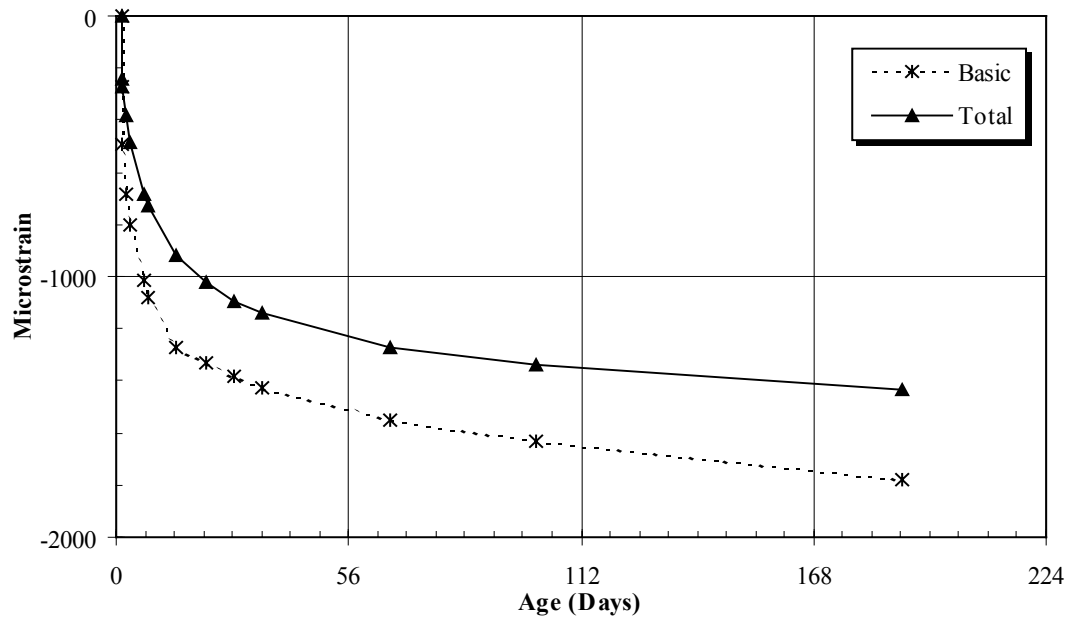


Figure 3.9. Creep Rig 4 Creep Strain (152-mm Diameter, Girder 1C, 20.7 MPa)

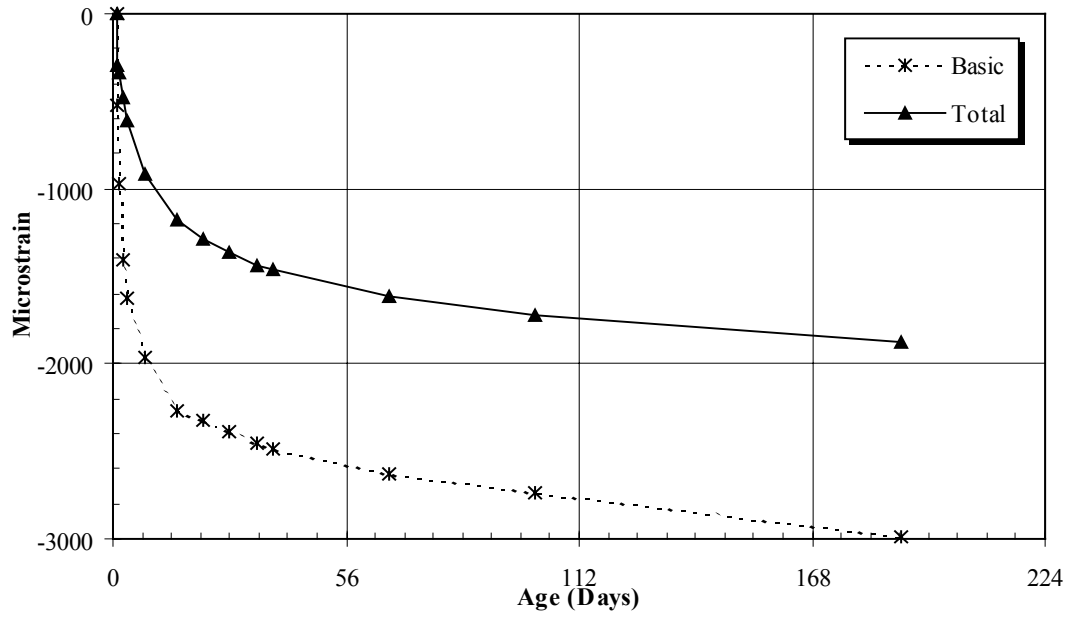


Figure 3.10. Creep Rig 5 Creep Strain (152-mm Diameter, Girder 1C, 27.6 MPa)

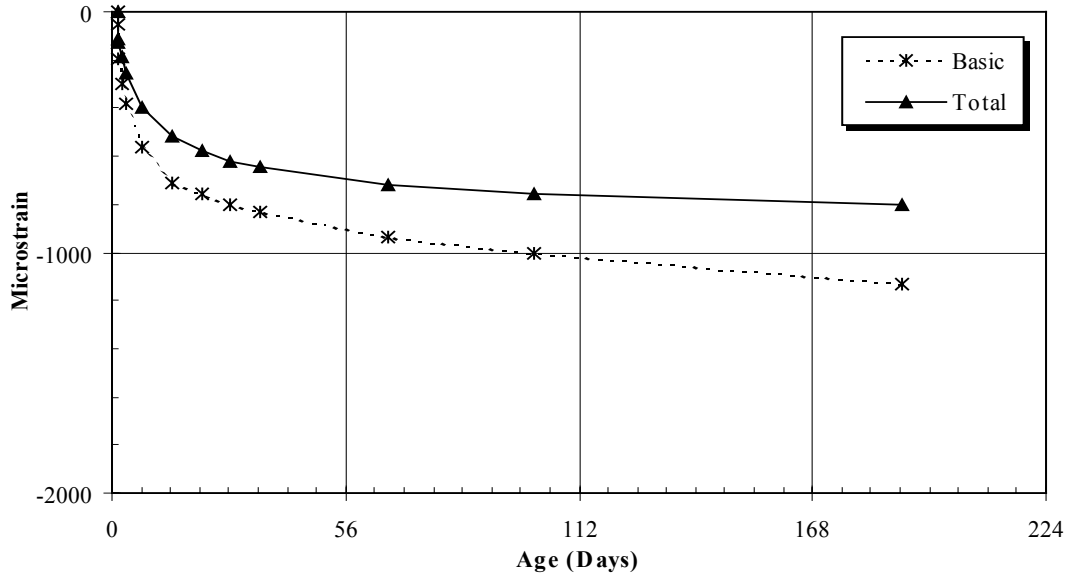


Figure 3.11. Creep Rig 6 Creep Strain (152-mm Diameter, Girder 1C, 13.8 MPa)

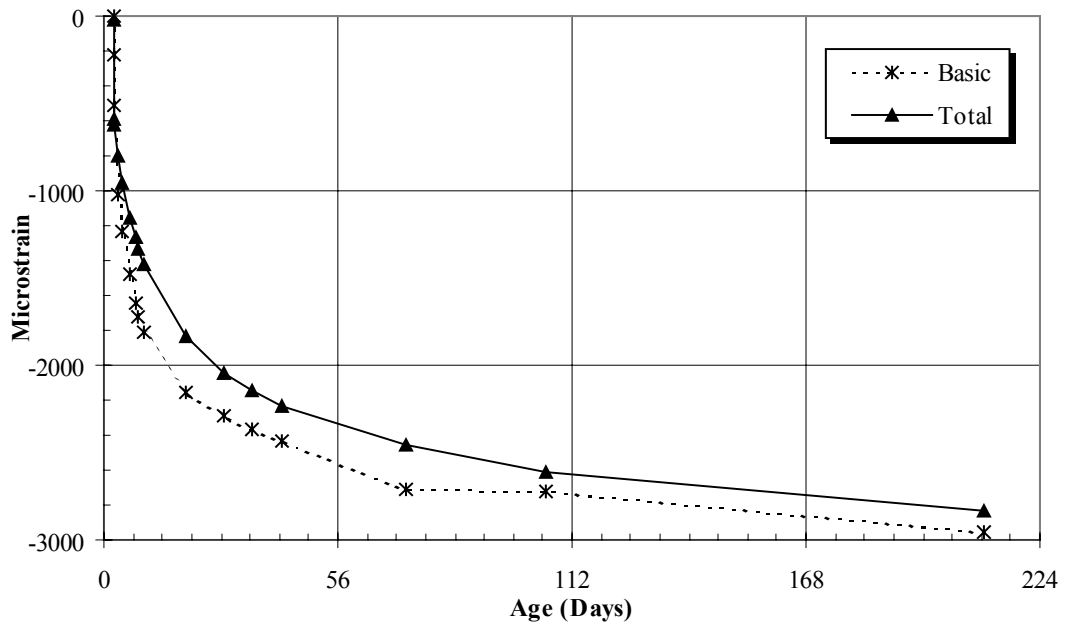


Figure 3.12. Creep Rig 8 Creep Strain (102-mm Diameter, Girder 2C, 26.7 MPa)

3.1.4 Creep Coefficient

The creep strains were normalized by the elastic strain of each creep rig listed in Table 3.3, yielding the history of the creep coefficient. These histories are shown in Figures 3.13 and 3.14 for the unsealed and sealed specimens, respectively. A trend can be seen in the grouping among the creep coefficients for the total creep specimens in Figure 3.13. The three smallest values are those for Creep Rigs 4, 5, and 6. These creep rigs were all loaded with specimens from Girder 1C casting and were loaded at the same time. The middle “group” is the single creep rig built from specimens from the Test Girder casting. The two largest values are those from Creep Rigs 1 and 8, both of which used specimens from the Girder 2C casting.

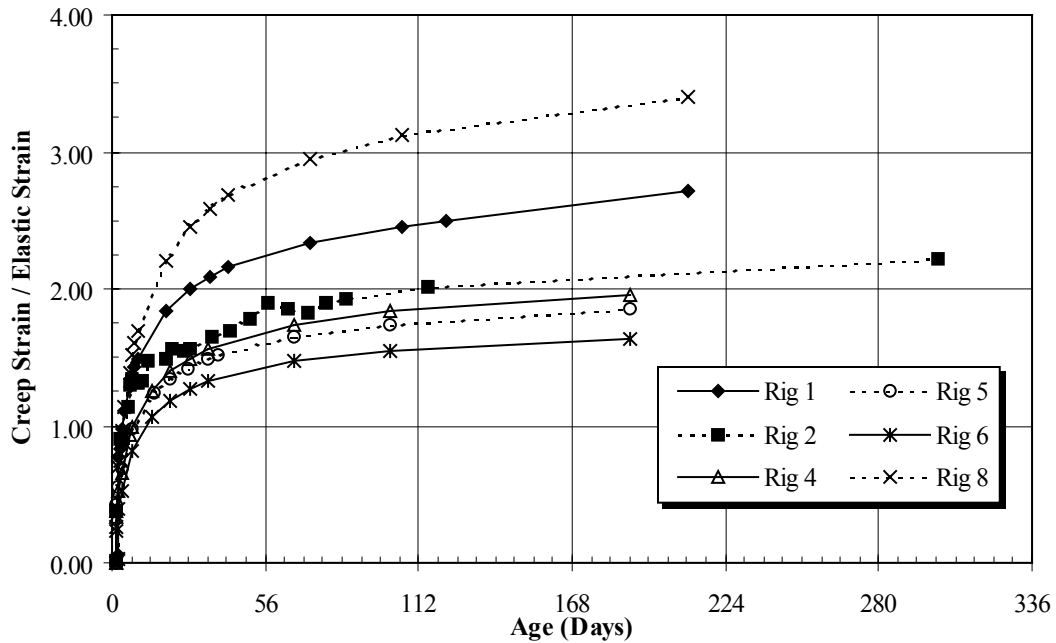


Figure 3.13. Total Creep, Creep Coefficients for Unsealed Specimens

A similar grouping exists in the sealed specimens in Figure 3.14, but it is not as distinct. The three Girder 1C creep rigs are grouped together, and the Test Girder creep rig is on its own and much lower than any of the others. The two Girder 2C creep rigs are no longer grouped together; however, Creep Rig 8 still predicts the highest value of the creep coefficient.

It is possible that these groupings are related to the maturity of the specimens at the time of loading in the creep rigs. The curing regime and time of loading were consistent for all specimens from the same casting, but differed between castings. The differences in curing would result in different maturities at loading, and likely the type of grouping seen here. The most pronounced variation in the curing process was in the sealed specimens because of difficulties with the coating process. This difference in curing could explain the anomalies seen only in the sealed specimens.

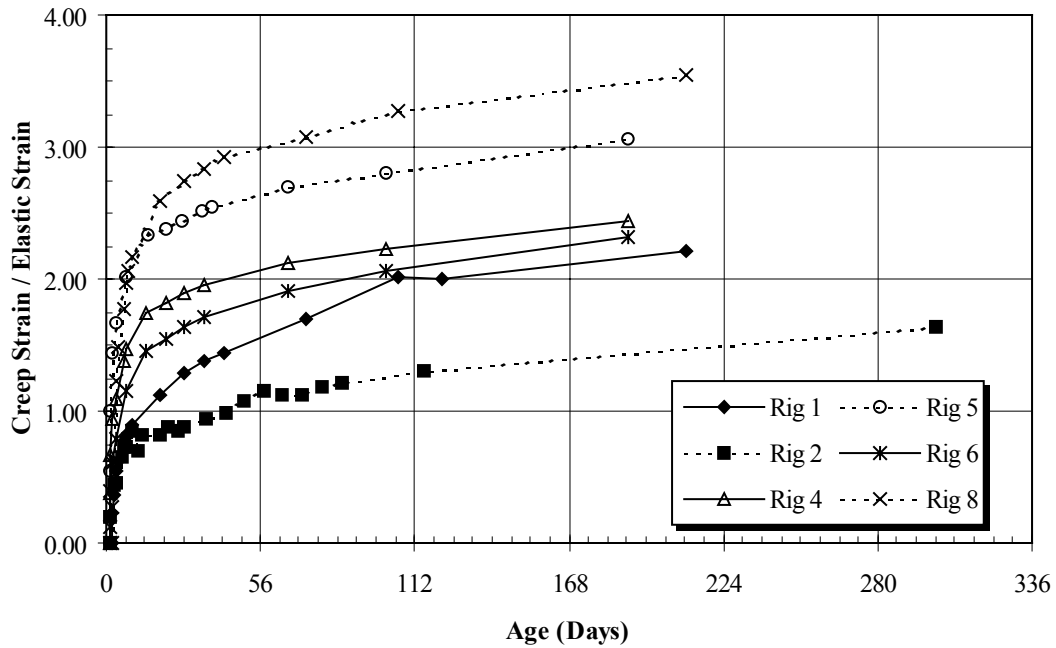


Figure 3.14. Basic Creep, Creep Coefficients for Sealed Specimens

Table 3.5 provides a summary of the creep coefficient and specific creep values calculated for each creep rig at the end of loading. The table reports the creep coefficient for both basic and total creep strains, but it reports only the specific creep values for total creep. There is reasonably good agreement between the total creep, creep coefficients for Creep Rigs 2, 4, 5, and 6, and especially in the specific creep values for these same creep rigs.

The most significant comparison is between the values for Creep Rigs 4, 5, and 6, which were all cast from girder 1C concrete. The specimens presumably have similar histories. The three total creep, creep coefficients range from 1.64 to 1.96, a variation of about 15 percent. The values calculated using the strains from the 102 mm x 304 mm (4 in x 12 in) diameter cylinders in Creep Rig 8 are much higher than any of the others,

predicting a specific creep of more than 0.15 microstrain per kN. Typical specific creep values do not exceed 0.10 microstrain/kN.

Table 3.5. Creep Coefficients and Specific Creep

Creep Rig	Total Creep Creep Coefficient	Basic Creep Creep Coefficient	Specific Creep (microstrain/ kN)
1	2.72	2.21	0.117
2	2.22	1.64	0.094
4	1.96	2.43	0.103
5	1.86	3.07	0.097
6	1.64	2.31	0.087
8	3.40	3.54	0.151

3.1.5 Summary of Creep Test Results

The results of the creep tests suggest that:

- The creep test results were likely sensitive to variations in cylinder maturity at the time of loading.
- To examine the influence of a particular variable, it is important that the early curing conditions remain the same for all of the cylinders.
- The total measured creep coefficient after 6 months of testing ranges from 1.64 to 2.72 for total creep of 152-mm (6-in) diameter cylinders. These values significantly exceed the value of 1.60 suggested for 68.9 MPa (10,000 psi) concrete by Nilson (1987).

3.2 SHRINKAGE TEST RESULTS

Four sets of two companion cylinders with shrinkage measurements were monitored for the analysis of the six creep rigs, one set of 152-mm (6-in) diameter cylinders for each of the three girders and one 102-mm (4-in) diameter set for Girder 2C.

Figures 3.15 to 3.18 show these free shrinkage strains measured using gauge studs attached to the sides of the specimens. Figure 3.19 provides the shrinkage strains in the Girder 1C cylinders shown in Figure 3.18, but measured from studs embedded in the ends. Table 3.6 provides a summary of the maximum shrinkage strain measured in each of these samples.

Table 3.6. Summary of Maximum Shrinkage Strain in Cylinders

Girder Sampled	Cylinder Diameter (mm)	Location of Gauge Studs	Figure	Maximum Shrinkage Strain
TEST	152	side	3.15	-370
2C	152	side	3.16	-570
2C	102	side	3.17	-570
1C	152	side	3.18	-570
1C	152	end	3.19	-860

The shrinkage measurements began at the same time that the creep rigs were loaded, approximately 1 day after casting. The basic shrinkage occurring between casting and loading, although it does affect the girders, does not affect the creep analysis since it occurs prior to any measurements on the loaded specimens. The basic shrinkage occurring thereafter does affect the creep behavior, however, and it is measured in the companion cylinders and subtracted from the unsealed specimens as part of the total shrinkage. Since it was not measured independently, it remains in the basic creep strain.

The 600 microstrain measured in the production girder cylinders (Table 3.6) is higher than would be expected in a high strength concrete; however, shrinkage takes

place primarily in the hydrated cement paste and an increase in the paste content would be expected to result in an increase in the shrinkage. The mix design used for these girders contains 36 percent cement paste, compared with conventional concrete mixes with approximately 25 to 30 percent paste. HPC often requires a higher paste content, and frequently uses silica fume.

The shrinkage strains measured in the 152-mm (6-in) diameter Test Girder cylinders (Figure 3.15) are smaller than those from cylinders cast from the other concrete batches. The three strain measurements from the production girder concrete are all in the range of about 600 microstrain (Figures 3.16 to 3.18), whereas the Test Girder shrinkage is less than 400 microstrain (Figure 3.15).

The tests took place under almost identical environmental conditions, and the same moisture conditions existed in the cylinders when testing began. However, they began at different times depending on when the creep rigs were loaded with their companion cylinders. This difference in timing could result in higher values of basic shrinkage being measured the earlier the test began. The increase in basic shrinkage would increase the total shrinkage.

The shrinkage measured from the gauge studs embedded in the ends of the cylinder (Figure 3.19) is significantly higher than that of the same cylinders measured from the side in Figure 3.18. The difference may be attributable to the shrinkage restraint at the edges provided by the cracks resulting from differential shrinkage through the depth of the cylinder. Also, a comparison of Figures 3.16 and 3.17 shows that the 102-mm (4-in) diameter specimens experience larger strains than the 152-mm (6-in) diameter cylinders at first, due to the smaller volume-to-surface ratio, but have the same maximum value of -575 microstrain.

Figures 3.15 to 3.18 show the curves fitted to the shrinkage strains measured from the sides of the companion specimens used for the creep analysis. The curve fit is of the form $\epsilon_{sh} = A \ln(t)$. The curves appear to predict the shrinkage strain well over the first

100 days, but then they consistently begin to over-predict the strains. This trend is most likely due to the time-function selected and the inability to find a single function to accurately describe the time-dependency of shrinkage. However, at 200 days, the largest difference between the fitted curve and the average of the specimens is approximately 60 microstrain. This difference is small (less than 6 percent) in comparison with the creep strains that are the focus of the analysis.

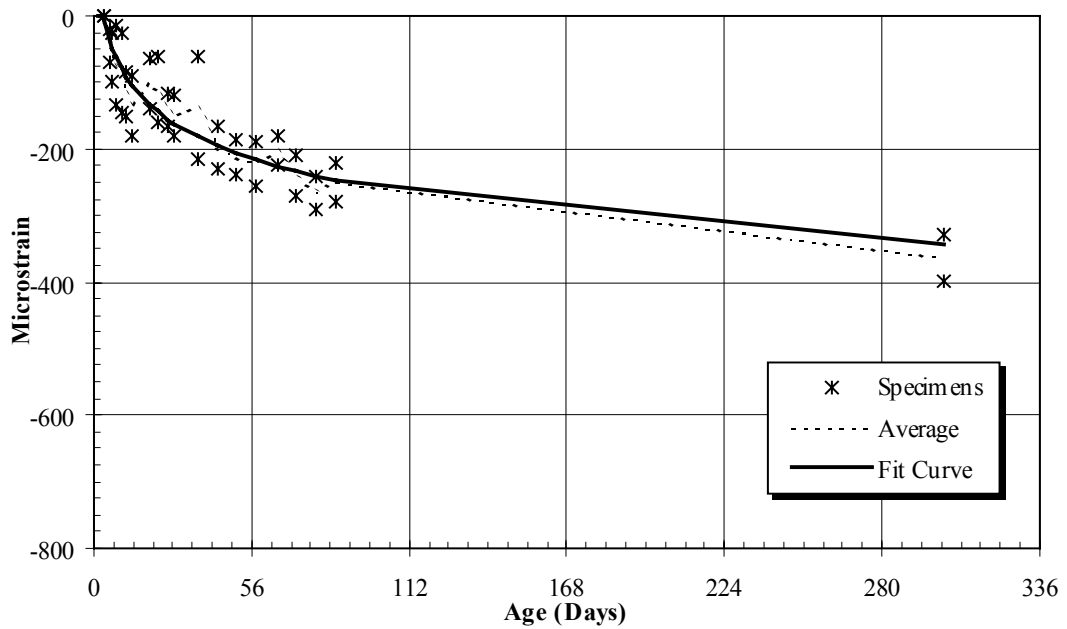


Figure 3.15. Shrinkage Strains of Test Girder Specimens (152-mm-Diameter)

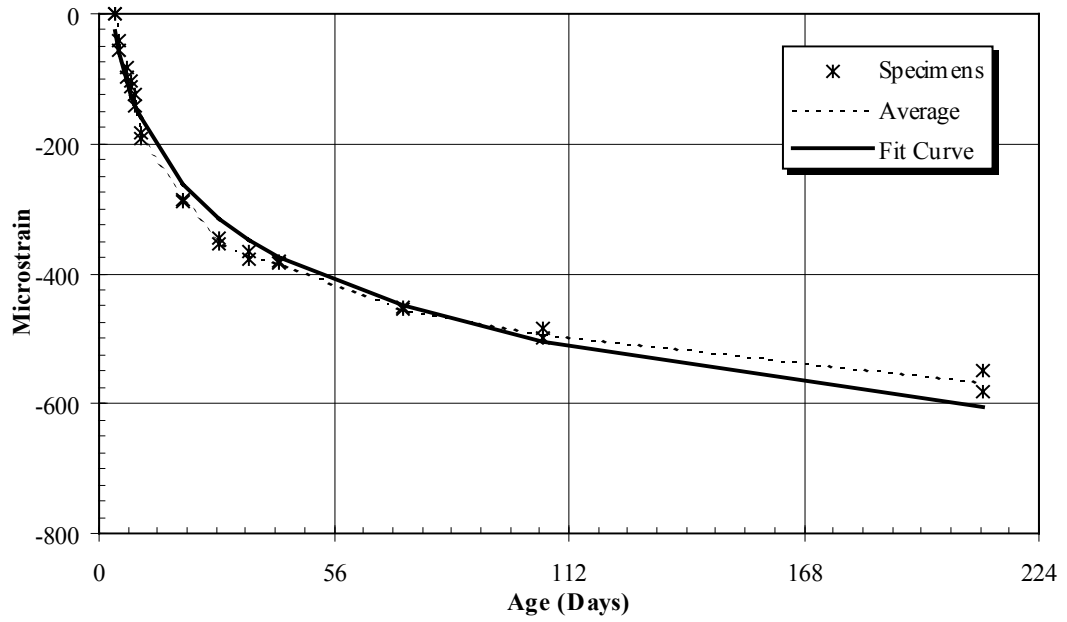


Figure 3.16. Shrinkage Strains of Girder 2C Specimens (152-mm Diameter)

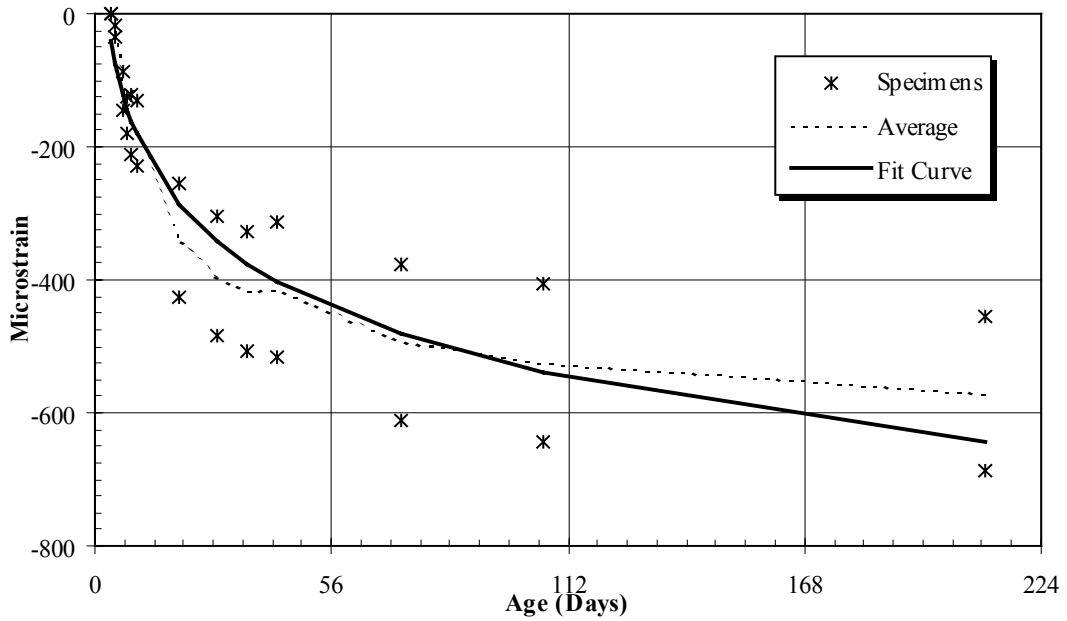


Figure 3.17. Shrinkage Strains of Girder 2C Specimens (102-mm Diameter)

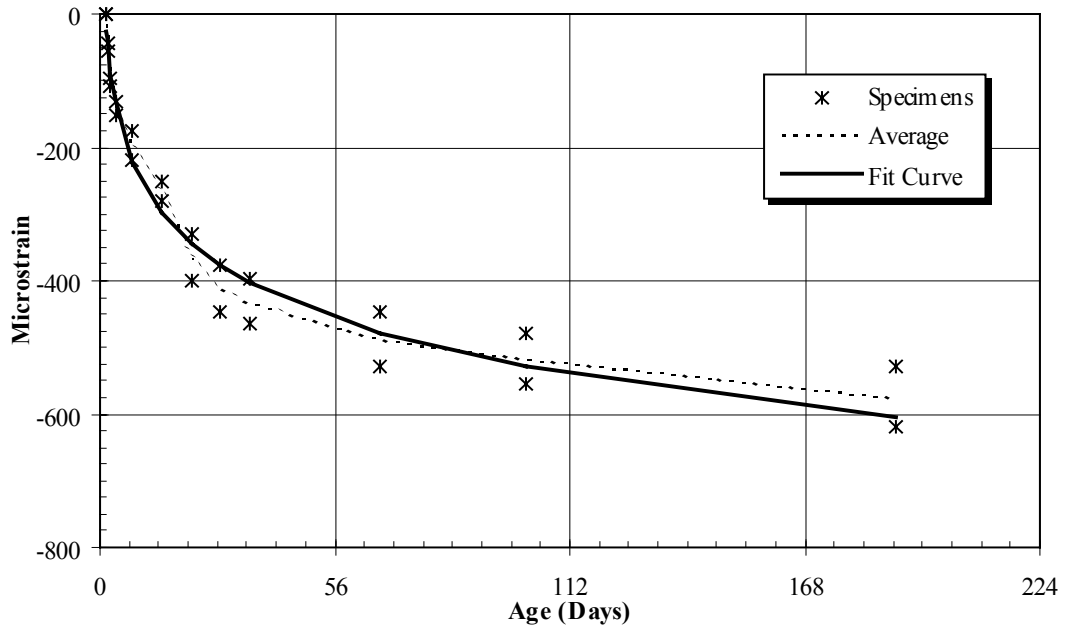


Figure 3.18. Shrinkage Strains of Girder 1C Specimens (152-mm Diameter)

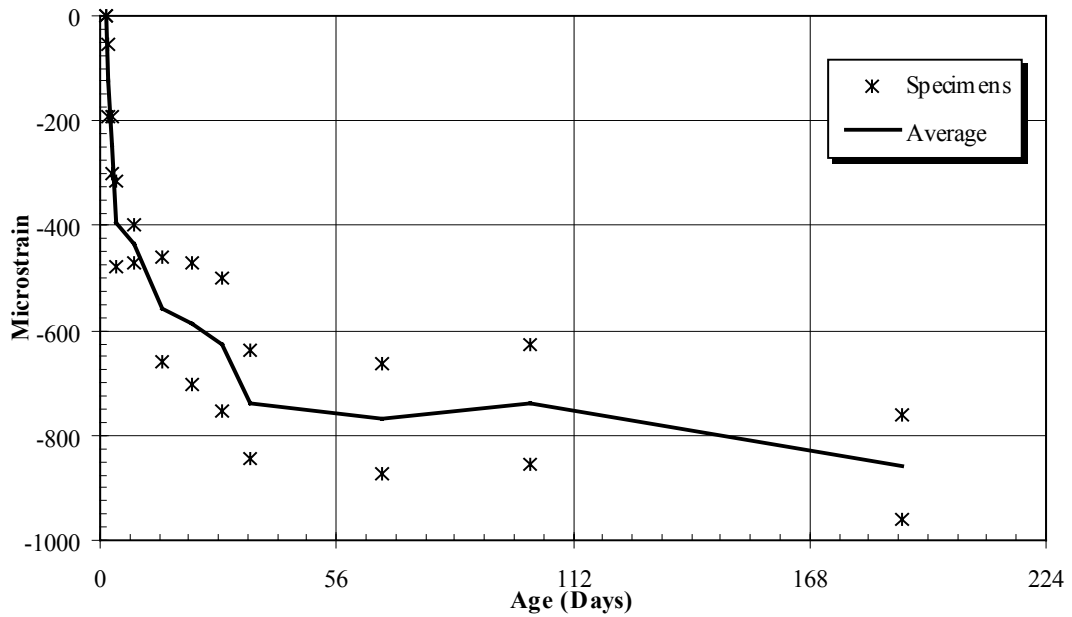


Figure 3.19. Shrinkage Strain from Ends in Girder 1C Specimens (152-mm Diameter)

Shrinkage was also measured on standard [76 mm x 102 mm x 406 mm (3 in x 4 in x 16 in)] shrinkage beams during the first few months using gauge studs embedded in their ends. The strains measured with the two types of specimens are compared in Figures 3.20 to 3.22; a summary of the maximum measured shrinkage in all specimens is provided in Table 3.7. The value of the beam shrinkage represents less than 3 months of shrinkage, whereas the cylinder strains represent at least 6 months of testing.

Table 3.7. Summary of Maximum Shrinkage Strain in Beams and Cylinders

Girder Sampled	Specimen Type	Location of Gage Studs	Maximum Shrinkage Strain
TEST	152 mm Cylinder	side	-370
TEST	Beam	end	-730
2C	152 mm Cylinder	side	-570
2C	102 mm Cylinder	side	-570
2C	Beam	end	-620
1C	152 mm Cylinder	side	-570
1C	152 mm Cylinder	end	-860
1C	Beam	end	-500

The testing of the Test Girder beams (Figure 3.20) did not begin until 7 days after casting (ASTM C157). During this time, the specimens remained in the fog room and the cement paste continued to hydrate, eliminating the majority of basic shrinkage leaving almost entirely drying shrinkage. However, the shrinkage at 78 days in the cylinders was still lower than that of the beams, -270 compared with -730 microstrain. As the beams have a much smaller volume-to-surface ratio, the drying shrinkage alone should be larger, but not of this magnitude. No explanation for this discrepancy has been found.

The effect of volume-to-surface area ratio can be seen again in Figure 3.21, which shows the shrinkage strains of the 102-mm and 152-mm (6-in and 4-in) diameter cylinders compared with the 76 mm x 102 mm x 406 mm (3 in x 4 in x 16 in) beams.

These specimens, in the order listed, have V/S values of 51 mm, 38 mm, and 20 mm (2.0 in, 1.5 in, and 0.77 in) and the shrinkage increases as V/S decreases. Figure 3.26 shows that the drying shrinkage measured from the ends of the beams is lower than that measured from the ends of the cylinders.

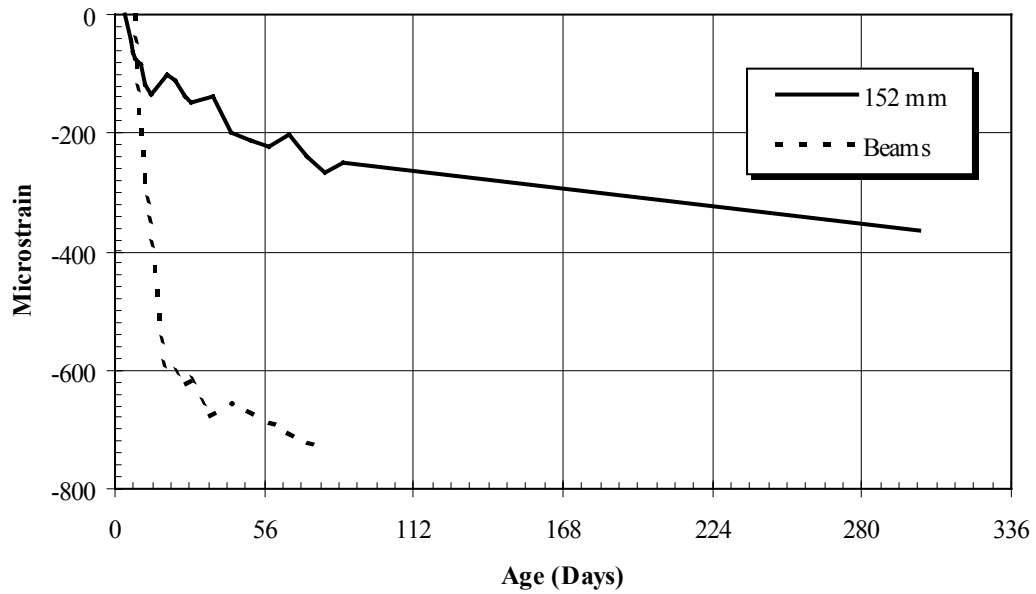


Figure 3.20. Shrinkage in Test Girder Cylinders and Beams

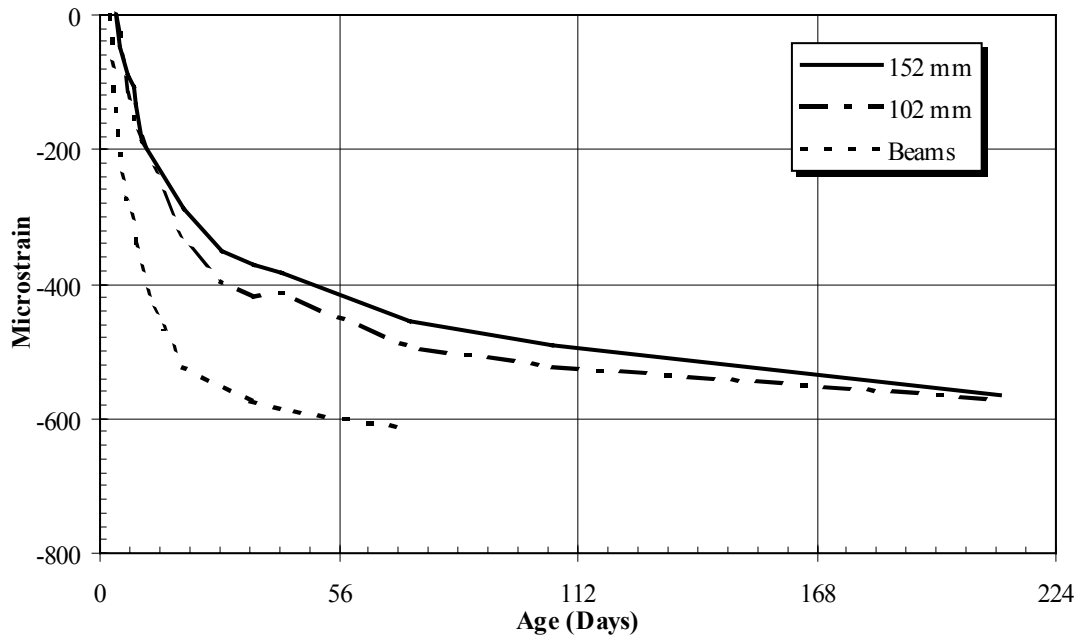


Figure 3.21. Shrinkage in Girder 2C Cylinders and Beams

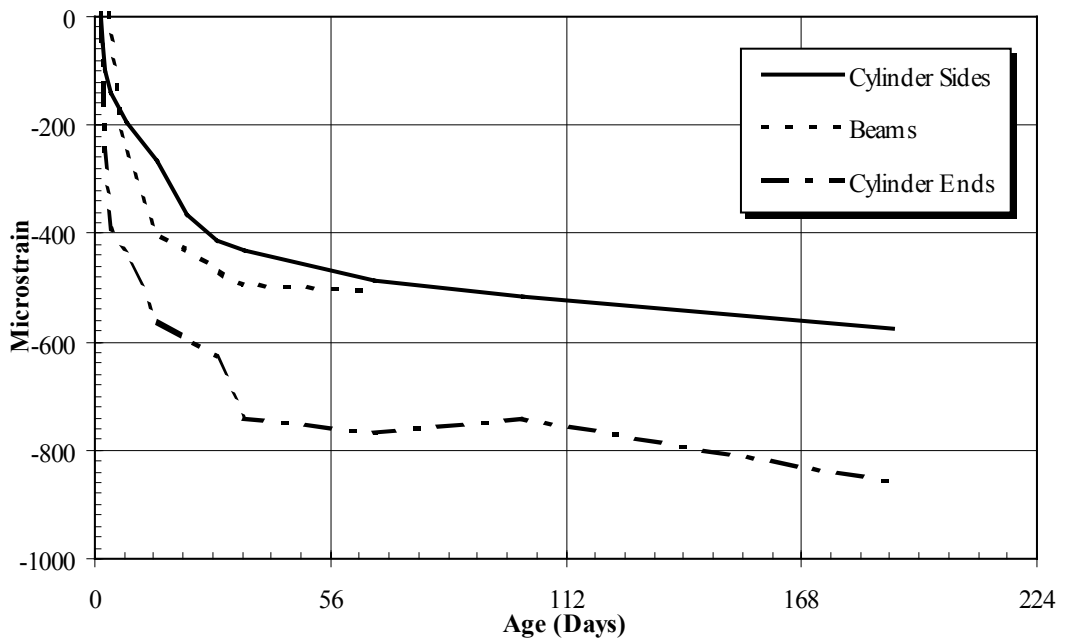


Figure 3.22. Shrinkage in Girder 1C Cylinders and Beams

The approach taken with the shrinkage tests was to provide the necessary information for the creep analysis. This meant that the testing for each batch of concrete began at several different times, depending on when the creep rigs were loaded. It did provide much of the necessary information for the creep analysis; however, as a result, it is very difficult to compare relative magnitudes of the shrinkage strain among concrete batches.

3.3 CONCRETE COMPRESSIVE STRENGTH

The measured concrete compressive strengths are summarized in Figure 3.23. The strength of the Girder 2C concrete exceeded that of the other two girders sampled. This difference may have been, in part, due to a difference in the curing regime for these specimens. The cylinders were left out of the insulated boxes for several hours longer than the other samples and, consequently, they never reached as high a temperature during the initial cure. A lower curing temperature is known to be beneficial to the long-term strength gain (Troxell et al., 1968). All batches of concrete exceeded the 56-day specified strength of 68.9 MPa (10,000 psi).

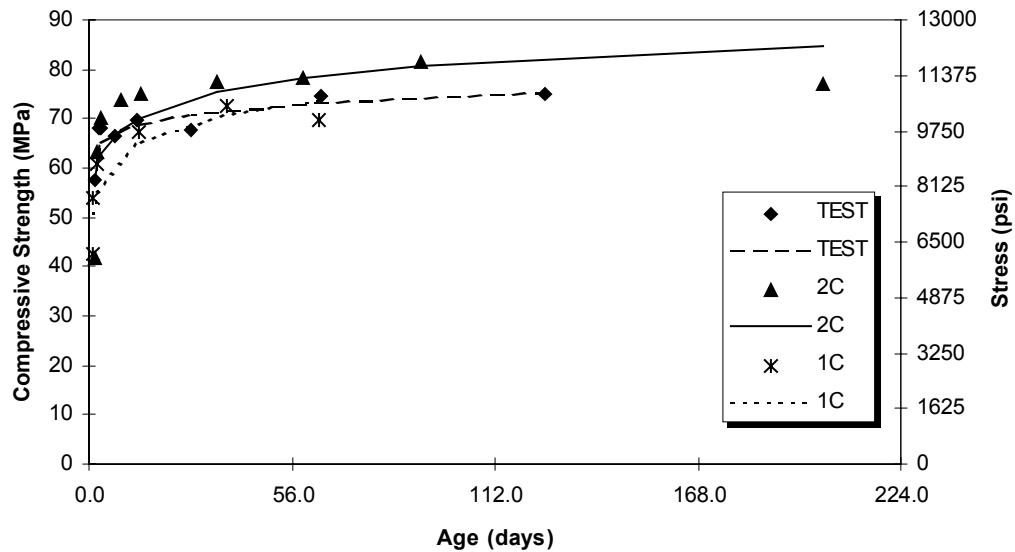


Figure 3.23. Concrete Compressive Strength

Figure 3.24 compares the compressive strengths measured in the laboratory with those measured on site by the fabricator for the two production girders. The specimens tested by the fabricator were match-cured with the sure-cure steam system. Those tested in the lab were cured as previously described (Chapter 2). The comparisons at an early age are complicated by the paucity of data from the fabricators tests. The 28-day strength for Girders 1C and 2C were higher for the fabricator's tests. The difference is most significant in the Girder 1C tests. At 56 days, the fabricator's specimens were almost 6.9 MPa (1000 psi) stronger than the laboratory specimens.

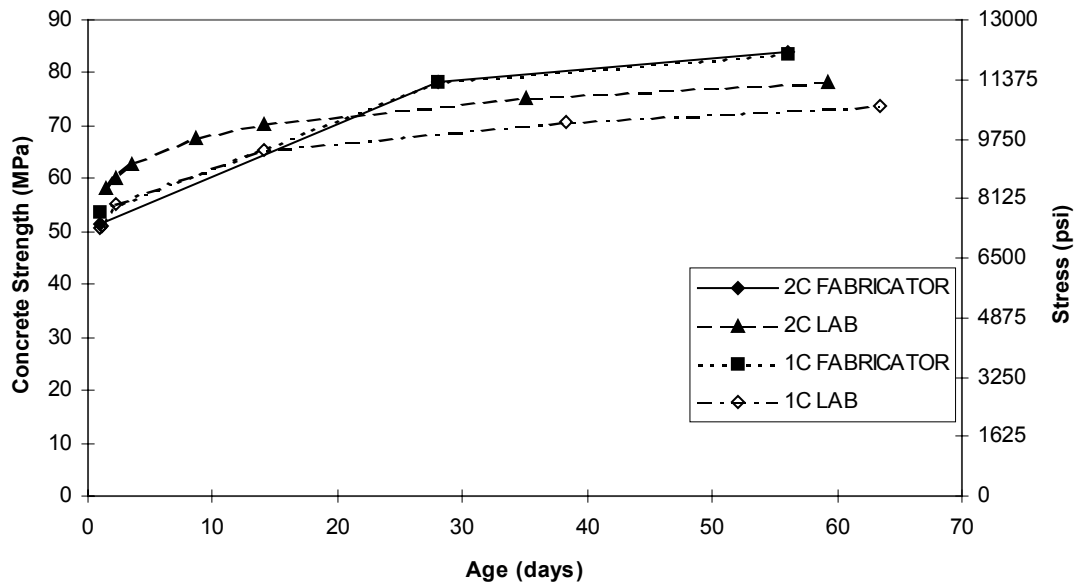


Figure 3.24. Onsite and Laboratory Measured Compressive Strength

3.4 CONCRETE MODULUS OF ELASTICITY

The modulus of elasticity was measured on specimens from all three girders. Figure 3.25 summarizes the results of these tests. Although the value measured for the Girder 1C samples at 56 days was 5 percent lower than that in the samples from Girder 2C and the Test Girder [34.5 GPa (5000 ksi) compared with 36.5 GPa (5300 ksi)], Girder 1C does reach the same value of elastic modulus in the long term as the Girder 2C samples. The specimens from both Girder 1C and 2C show a value of the elastic modulus of 37.9 GPa (5500 ksi) at 180 days.

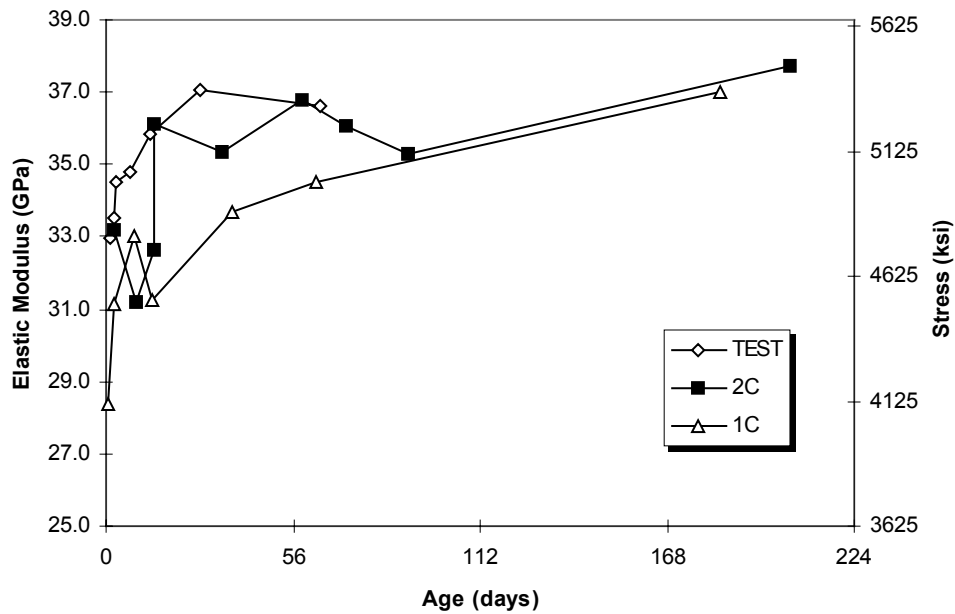


Figure 3.25. Concrete Modulus of Elasticity

3.5 CONCRETE TENSILE STRENGTH

The split-cylinder tensile strengths are summarized in Figure 3.26. Tensile strength is often assumed to be related to the square root of compressive strength. Although the compressive strength tests were lower in the short term for the Girder 2C specimens, this is not the case for the tensile strength tests. The relation used in the ACI 318-95 *Building Code and Commentary* (ACI, 1995) suggests that the tensile strength, f_{ct} , is equal to 6.7 times the square root of the compressive strength. The measured values of tensile and compressive strength at 56 days suggest coefficients of approximately 7.8 and 8.1 for the concrete from Girders 1C and 2C, respectively. These values are slightly higher than that suggested by ACI, as has been noted in the past for high strength concrete (Neville, 1995).

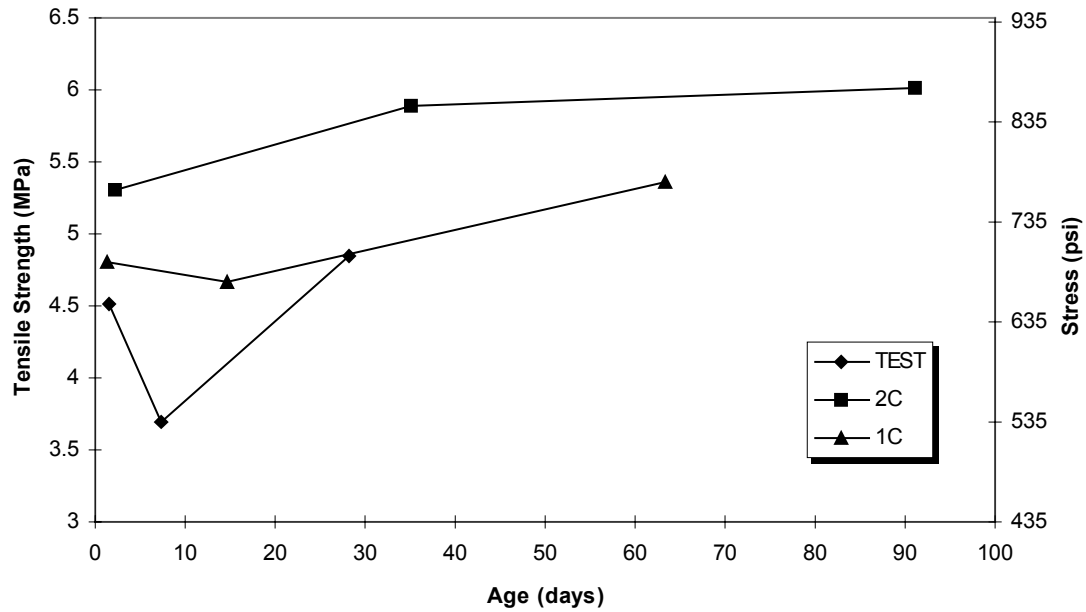


Figure 3.26. Concrete Tensile Strength

3.6 CONCRETE COEFFICIENT OF THERMAL EXPANSION

The coefficient of thermal expansion was measured for all three batches of concrete. Figure 3.27 fits a trend-line to the data from the Test Girder samples. The slope of this line is the coefficient of thermal expansion for the concrete, calculated to be of 10.6 microstrain/°C (5.9 microstrain/°F). The same procedure was followed for the concrete from the other two girders. Figure 3.28 shows the results from the Girder 2C samples. It suggests a coefficient of 9.7 microstrain/°C (5.4 microstrain/°F). Figure 3.29 is that for Girder 1C concrete; it has a coefficient of thermal expansion equal to 10.1 microstrain/°C (5.6 microstrain/°F).

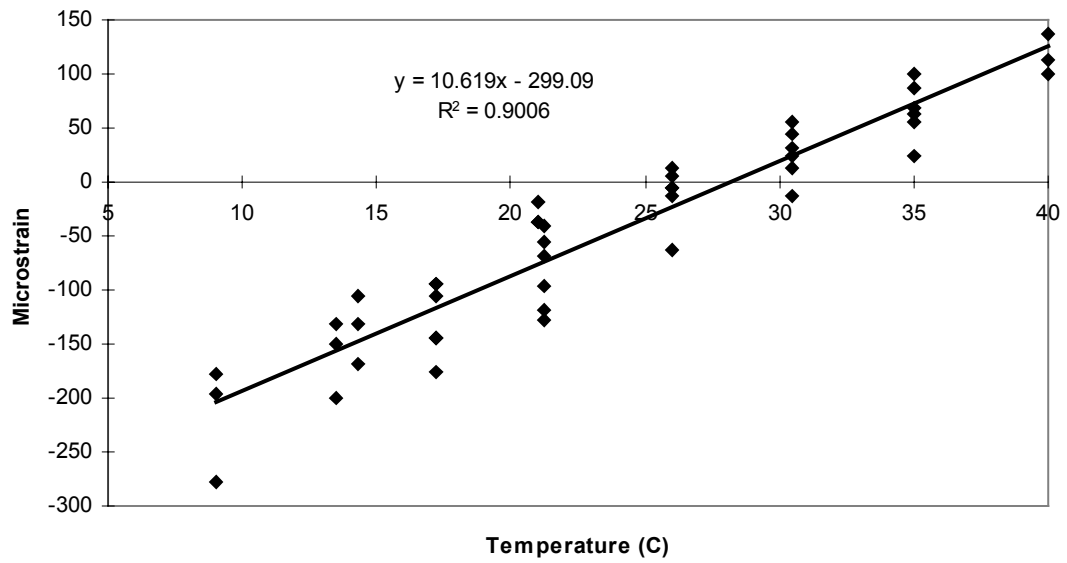


Figure 3.27. Test Girder Concrete Coefficient of Thermal Expansion

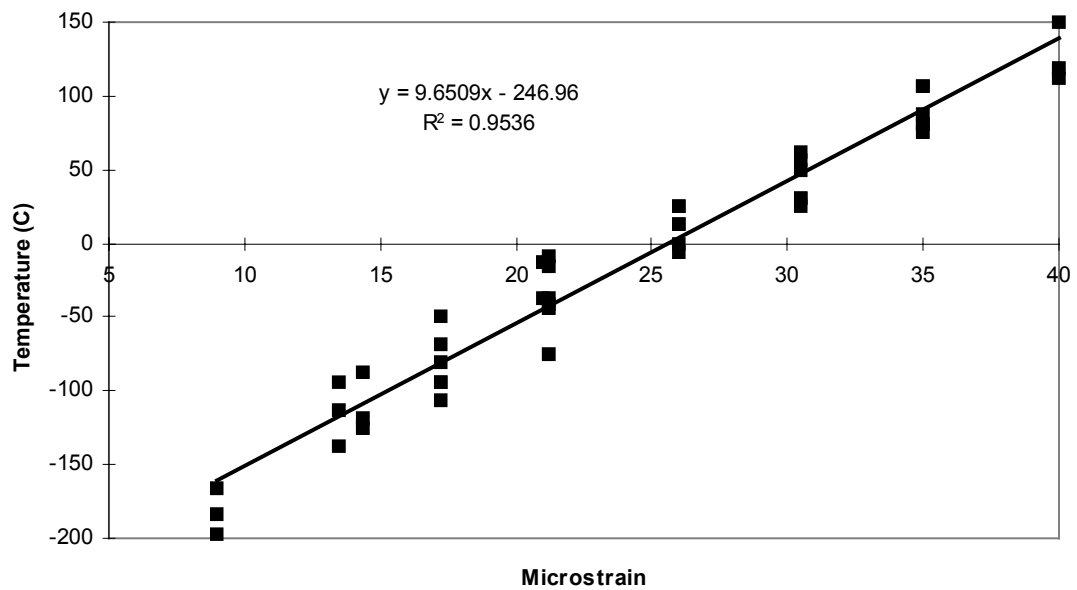


Figure 3.28. Girder 2C Concrete Coefficient of Thermal Expansion

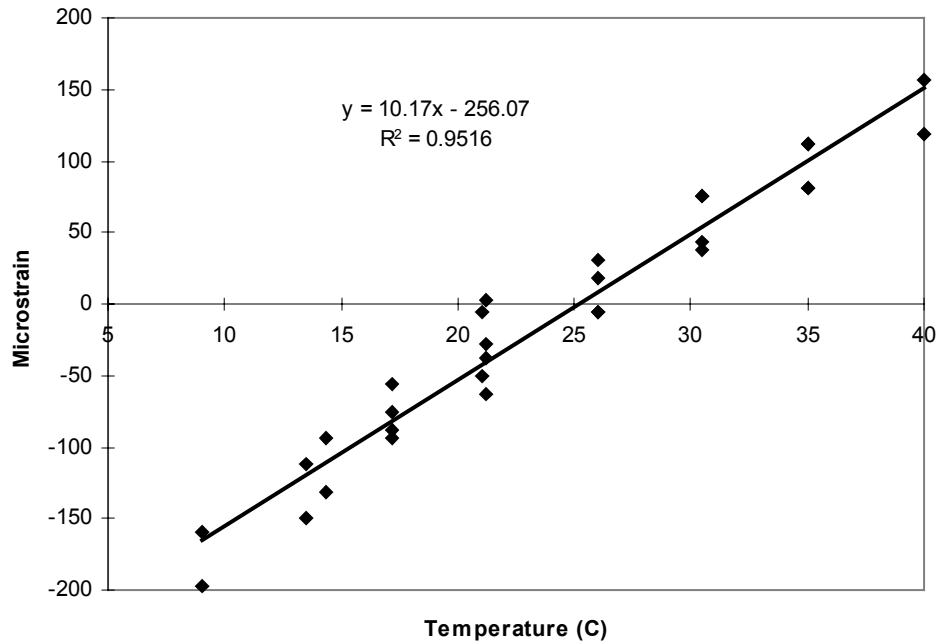


Figure 3.29. Girder 1C Concrete Coefficient of Thermal Expansion

Cement paste has a coefficient of thermal expansion that is higher than aggregate and usually ranges from about 10.8 to 21.6 microstrain/°C (6 to 12 microstrain/°F). The specimens tested from the Test Girder, and Girders 2C and 1C, have a range of 9.7 to 10.6 microstrain/°C (5.4 to 5.9 microstrain/°F). These results are consistent with the high paste content in this mix (Neville, 1995).

3.7 DURABILITY

The durability characteristics for the HPC mix were evaluated by performing freeze-thaw resistance tests (AASHTO T 161), chloride ion penetration tests (AASHTO T 277), and chloride penetration tests (AASHTO T 259). Each test was performed by WJE with samples taken by the fabricator.

3.7.1 Freeze-Thaw Resistance

None of the three samples that were tested indicated that any damage was caused by the cyclic freezing and thawing. This conclusion was reached by subjecting the specimens to approximately 300 cycles of freezing and then thawing, while measuring the relative dynamic modulus after roughly every 40 cycles.

3.7.2 Chloride Ion Penetration

The average coulomb value for the two specimens tested was 1010 coulombs. This value was considered as meeting the 1000 coulomb specification due to the high variability (12.3 percent) and inaccuracy of the test method.

3.7.3 Chloride Penetration (Ponding Test)

The four samples tested showed that the HPC has a very low chloride permeability and would be expected to have a longer service life when compared with identically exposed heat-cured conventional concretes.

CHAPTER 4

DISCUSSION OF RESULTS OF CREEP TESTS

The previous chapter presented the results of the materials testing program. The characteristics of the six loaded creep rigs are summarized in Table 3.1. This chapter discusses the behavior observed during the creep tests.

4.1 MEASUREMENT RELIABILITY

Measurements in the creep and shrinkage tests were subject to several sources of potential error, which are discussed in this section. Their effects were counteracted by the introduction of a moderate degree of redundancy. Two sealed and unsealed cylinders were loaded identically and measured independently in each creep rig, except in those containing 102 mm x 304 mm (4 in x 12 in) cylinders. Only two of these cylinders (one sealed and one unsealed) could be placed in a creep rig without risking instability. Further redundancy was introduced by installing four sets of gauge studs on most cylinders. A single strain estimate needs data from two diametrically opposing sets of studs, thus two independent measurements were available for each cylinder. Exceptions were the majority of the Test Girder cylinders, which were furnished with only two sets of gauge studs.

The most common correction was made due to difficulties in reading the dial gauges of the Whittemore gauge. It uses two dials, for 0.25 mm (0.01 in) and 0.0025 mm (0.0001 in). The first of these gauges can be difficult to read, and a reading error of 0.25 mm (0.01 in) causes a strain error of 1000 microstrain. Fortunately, a discrepancy as large as this can be easily detected, given the trend in the strain evident from previous readings. The appropriate adjustments were made and recorded.

Problems also existed with the spring system within the mechanical gauge. Minor jostling of the gauge resulted in different initial and final calibration values. If the time when the bump occurred was recorded, all measurements taken before the bump were

analyzed using the initial calibration, and the final calibration was used for all of those following it. In cases when the occurrence was not noted, but a large discrepancy in the calibration readings existed, it was necessary to determine when it had occurred. This identification was done using the trend evident from previous measurements and the knowledge of the order in which the readings were taken.

On the first set of tests from the Test Girder samples, the gauge studs frequently fell off. If this occurred immediately after a reading was taken, the stud was reattached, a new measurement was made, and the event was recorded. The analysis was modified to use the first reading after reattaching the stud for the new initial length. Any subsequent strain measured was added to the value of the strain from the last reading prior to the stud falling off. If the gauge stud fell off between readings, the same procedure was followed except that the strain when it was reattached was not known. Linear extrapolation using the previous two values was used to predict this value. The data from a pair of gauge studs was occasionally missing for a variety of reasons. If data from two sets of diametrically opposing gauge studs could not be averaged to obtain one measurement, no data were reported. This problem did not significantly affect the creep rig loaded with cylinders from the production girders.

Three measurements were made for each creep rig. Readings were taken initially, after pumping, and after the oil pressure in the jack had been released. Some variation occurred in the load between readings due to the shortening of the cylinders. This factor was compensated for by reapplying the load every time a reading was taken. The largest change in strain as a result of releasing the pressure from the jack was 25 microstrain, but typically, it was less than 5 microstrain. The “after pumping” readings are used for the analysis because of this effect and the fact that the load is known most reliably while the jack is still in place.

4.2 SEALED AND UNSEALED CYLINDER STRAINS

In Creep Rig 5, the magnitude of the total strains in the sealed cylinders significantly exceeded the magnitude of the total strains in the unsealed cylinders (Fig. 3.4). In three other creep rigs (4, 6, and 8), the total strains in the sealed and unsealed cylinders were within 200 microstrain of each other (Figs. 3.3, 3.5, and 3.6). These results were unexpected, because one expects the creep strains in an unsealed cylinder to significantly exceed the creep strain in a sealed cylinder.

A consequence of this unexpected behavior is that the inferred basic creep strain exceeded the total creep strain for four of the six creep rigs (Figs. 3.9 to 3.12). The unexpected behavior can be attributed primarily to three factors: (1) the influence of variations in curing conditions on creep, (2) the influence of variations in curing conditions on initial elastic shortening, and (3) the inability to subtract the basic shrinkage component of the sealed specimen strains to obtain actual basic creep.

4.2.1 Effect of Curing Conditions on Creep

The unsealed cylinders were removed from the insulated boxes only a brief time before the gauge studs were attached and the cylinders were loaded in the creep rigs. In contrast, the sealed specimens were removed several hours before being loaded in the creep rigs. This removal was necessary to coat the sealed specimens with the epoxy to form the moisture seal. Without their insulation, the cylinders were unable to maintain their high temperature due to hydration. The lower temperature decreased the rate of hydration and maturity gain and, consequently, the strength and elastic modulus of the concrete in the sealed cylinders.

The consequences of this inconsistency are most visible in the sealed and unsealed cylinders in Creep Rig 5, in which Girder 1C specimens were loaded to 27.6 MPa (4000 psi). Figure 4.1 shows the average total strains, in microstrain, for the two types of cylinders. Because the modulus of elasticity of the sealed specimens was lower, the

sealed cylinder underwent a larger initial elastic response to the same applied stress (1500 versus 1220). During the first week, the concrete in the sealed specimens continued to hydrate and gain strength, and the difference in the strains measured for a given time interval during this first week decreased from 44 to 20 percent. After the first week, this trend reversed, and the unsealed specimens began to gain more strain during each interval than the sealed specimens.

It is perhaps not surprising that the largest discrepancies between total and basic creep strains are found in Creep Rigs 4, 5, and 6. All these rigs hold cylinders from Girder 1C. The difference between the curing regimes for the sealed and unsealed specimens would be expected to be the same for each creep rig.

4.2.2 Effect of Curing Conditions on Elastic Shortening

The elastic shortening was subtracted from both the sealed and unsealed cylinder strains. However, this subtraction is not strictly correct for the sealed cylinders because the sealed cylinders were less mature at the time of loading. Their elastic modulus was lower, and the corresponding initial strain was higher than that of the unsealed cylinders (1800 versus 1220, Figure 4.1). By underestimating the elastic strain of the sealed cylinders, the computed basic strain was too large. The computed value of basic strain probably included some elastic strain.

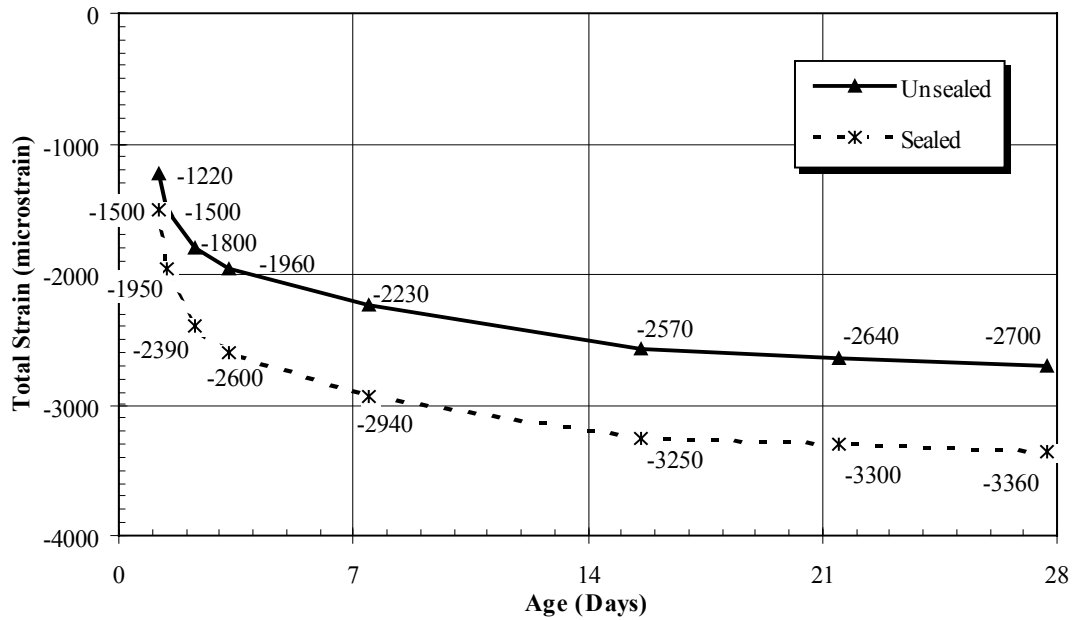


Figure 4.1. Creep Rig 5 Total Strains During First 28 Days

4.2.3 Effect of Basic Shrinkage

The different curing regimes applied to the sealed and unsealed specimens affected the relative values of both the total strains and the creep strains. In contrast, the inclusion of basic shrinkage in the basic creep contributes only to the discrepancy between the basic and total creep strains. One can simplify total strain as being composed of five components: initial elastic, basic and drying shrinkage, and basic and drying creep. All five are present in the unsealed specimens, but the drying shrinkage and creep strains are not included in the strains of the sealed cylinders.

The shrinkage measured in the companion cylinders and subtracted from the unsealed specimens contains both the basic and drying shrinkage, leaving only the basic and drying creep. No independent measurement of the basic shrinkage was made. Therefore, such a measurement cannot be subtracted from the sealed specimens, leaving

both the basic shrinkage and creep components in what is meant to model only basic creep. This factor tended to make the computed basic creep too large.

4.3 CREEP COEFFICIENTS

Although the relative magnitudes of the basic and total creep strains are reversed for the Girder 1C creep rigs, the difference is attributable to variations in curing conditions for the sealed and unsealed specimens. Therefore, the two sets of cylinders (sealed and unsealed) can be studied individually.

4.3.1 Unsealed Cylinders

The magnitude of the creep strain is expressed as the product of the initial elastic strain and the creep coefficient, or the product of the specific creep and the applied stress. In either case, the strains are modeled as being linearly related to the applied stress. Therefore, assuming that the creep prediction value is the same for all cylinders cast from the same concrete, and that all cylinders are exposed to the same environmental conditions, the creep strains from the three sets of 152-mm (6-in) diameter Girder 1C cylinders (Creep Rigs 4, 5, and 6) shown in Figure 4.2 should be proportional to the level of stress applied. This is approximately the case. After 189 days, the strains in the cylinders stressed to 13.8, 20.7, and 27.6 MPa (2000, 3000, and 4000 psi) were in the proportion 1.0:1.79:2.34, which is close to the expected ratio of 1.0:1.5:2.0.

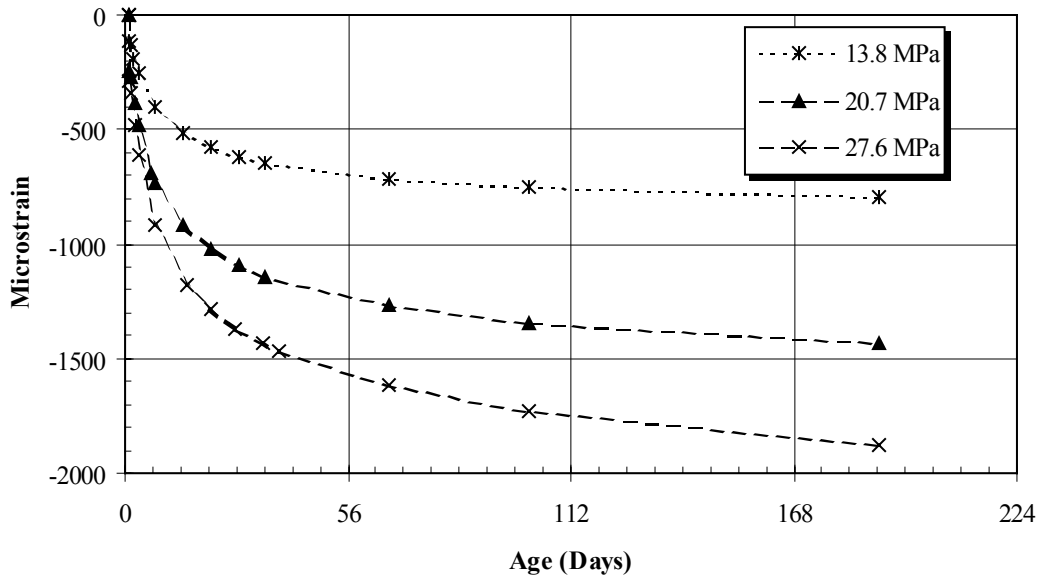


Figure 4.2. Effect of Applied Stress Level on Total Creep Strain (Girder 1C)

The linearity of the relationship may have been affected by stressing the concrete into the range where this linear relationship no longer holds true. The exact boundary of the range of linearity is not known with certainty. It has been suggested that the boundary is as low as 0.35 of the compressive strength at the time of loading (Troxell et al., 1968), and as high as 0.70 (Han and Walraven, 1996). The measured strength of specimens cast from the same concrete as these cylinders, and cured in the same manner, was approximately 53.8 MPa (7800 psi) at loading. This strength corresponds to applied stress-to-compressive strength ratios of 0.26, 0.38, and 0.51 for stress levels of 13.8, 20.7, and 27.6 MPa (2000, 3000, and 4000 psi). These ratios are consistent with limited non-linearity.

The creep coefficients corresponding to the creep strains in Figure 4.2 are shown in Figure 4.3. At day 189, the creep coefficient for the unsealed specimens ranged from 1.64 to 1.96.

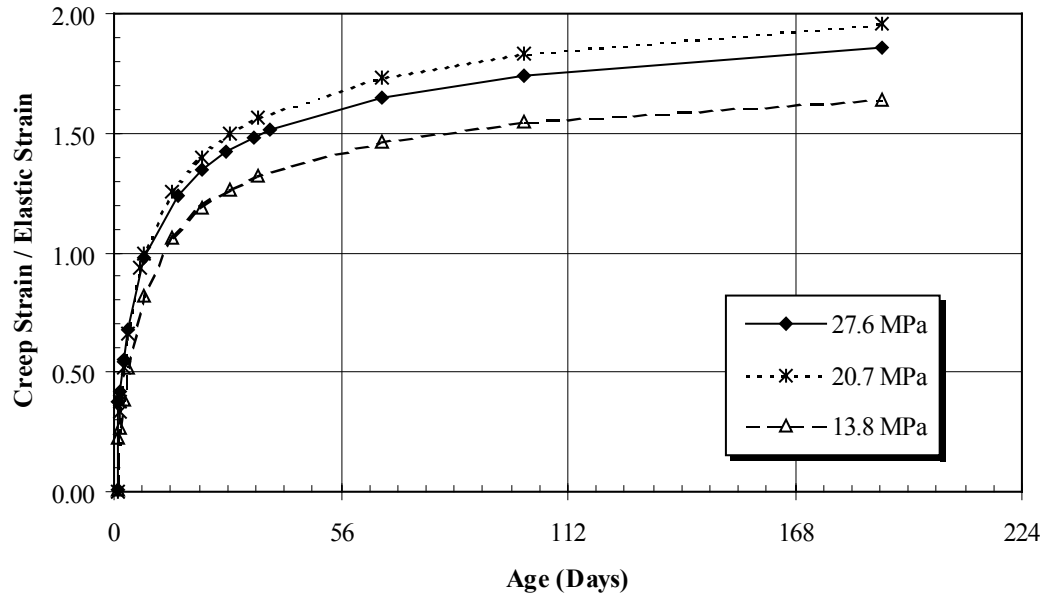


Figure 4.3. Effect of Stress Level on Creep Coefficient Using Total Creep Strain (Girder 1C)

4.3.2 Sealed Cylinders

The creep coefficients for these three creep rigs are shown in Figure 4.4. At day 189, the creep coefficient for the sealed cylinders ranged from 2.31 to 3.1. The increase in creep coefficient with strain is consistent with possible non-linearity in the concrete. The exact strength of the sealed cylinders at the time they were loaded is not known because of variations in curing conditions. If the actual strength of the sealed cylinders is lower than 53.8 MPa (7800 psi), then both the cylinders loaded to 20.7 and 27.6 MPa (3000 and 4000 psi) have stress-strength ratios that exceed the values of 0.38 and 0.51 for the unsealed cylinders.

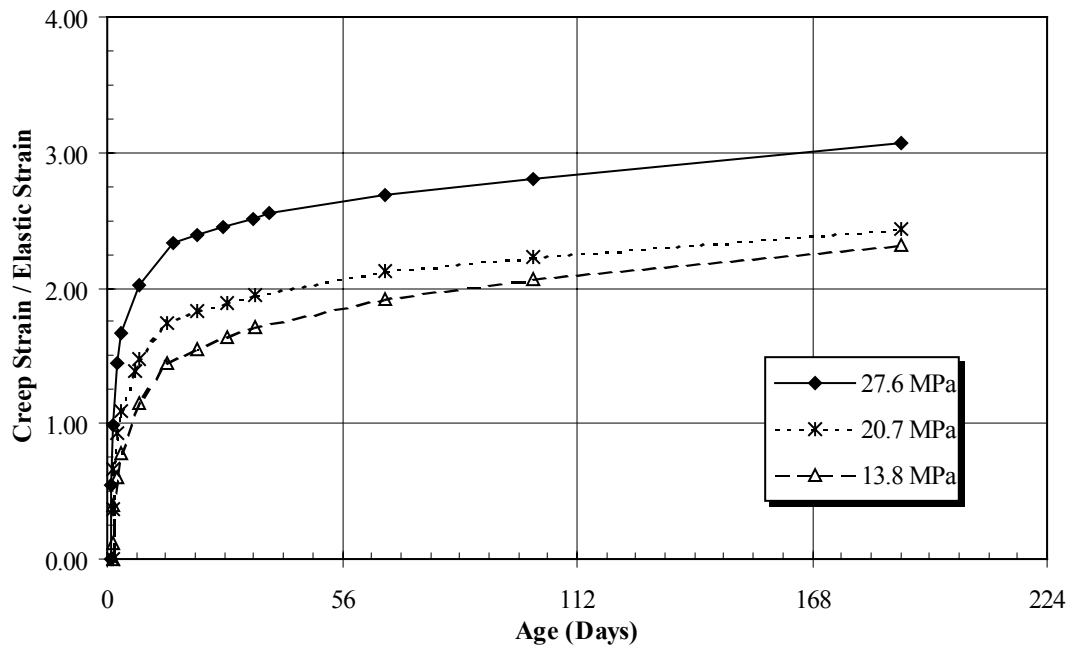


Figure 4.4. Effect of Stress Level on Creep Coefficient Using Basic Creep Strain (Girder 1C)

It was suggested previously (Section 4.2) that the value of elastic shortening that was subtracted from the basic creep strains was too small, and the creep coefficients are, therefore, too high. This error is compounded by normalizing by a value of elastic strain that is too small.

4.4 VOLUME-TO-SURFACE AREA RATIO

The total creep strains contain both basic and drying creep. It would be desirable to separate the drying creep from the total creep to examine the effect of the volume-to-surface area ratio, since it influences only the drying creep. This separation could be done by independently measuring the basic creep in sealed specimens at the same applied stress level and taking the difference between the basic and total creep. However, the basic

creep measured also contains a basic shrinkage component of unknown magnitude, and this separation procedure will under-predict the drying creep by an indeterminate amount.

A measure of the effect of the volume-to-surface ratio can be determined from the total creep strains in the 102-mm and 152-mm (4-in and 6-in) diameter unsealed cylinders loaded to the same applied stress, as shown in Figure 4.5. Each unsealed cylinder contains the basic and drying creep components, and since both are cast from the same concrete and are loaded to approximately the same level, the basic creep strains should be almost identical. Therefore, the difference between the total creep strains of the 102-mm (4-in) diameter cylinders and the 152-mm (6-in) diameter cylinders yields the difference in drying creep. The total creep strains are 2260 microstrain for the 152-mm (6-in) diameter and 2840 microstrain for the 102-mm (4-in) diameter. As expected, the drying creep strain is higher (by 580 microstrain) for the 102-mm (4-in) diameter cylinder with a smaller volume-to-surface area ratio.

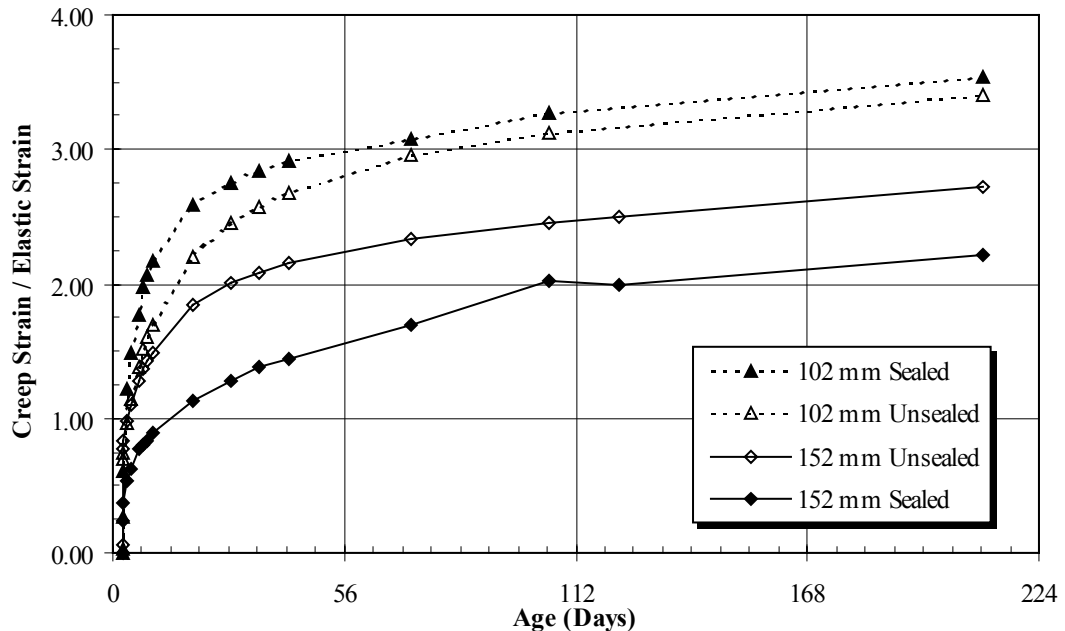


Figure 4.5. Effect of Volume-to-Surface Ratio on Creep Strain

The difference in strains is quite high, over 20 percent of the total creep strain in the 102-mm (4-in) diameter cylinder. This difference can be attributed to two factors. First, the basic creep strains were not equal for the different size specimens. Second, as was the case with the sealed specimens, a variation in the hydration temperatures between the specimens may have led to a lower maturity and, consequently, lower strength and higher strains. The unsealed specimens were all stored in the insulated boxes for approximately the same length of time from casting; however, it appears that the smaller thermal mass of the 102-mm (4-in) diameter cylinders compared with the 152-mm (6-in) diameter prevented these specimens from reaching as high a temperature during hydration. The difference in temperature is shown in the temperature histories in Figure 4.6 measured with a thermocouple from both size specimens while inside the boxes.

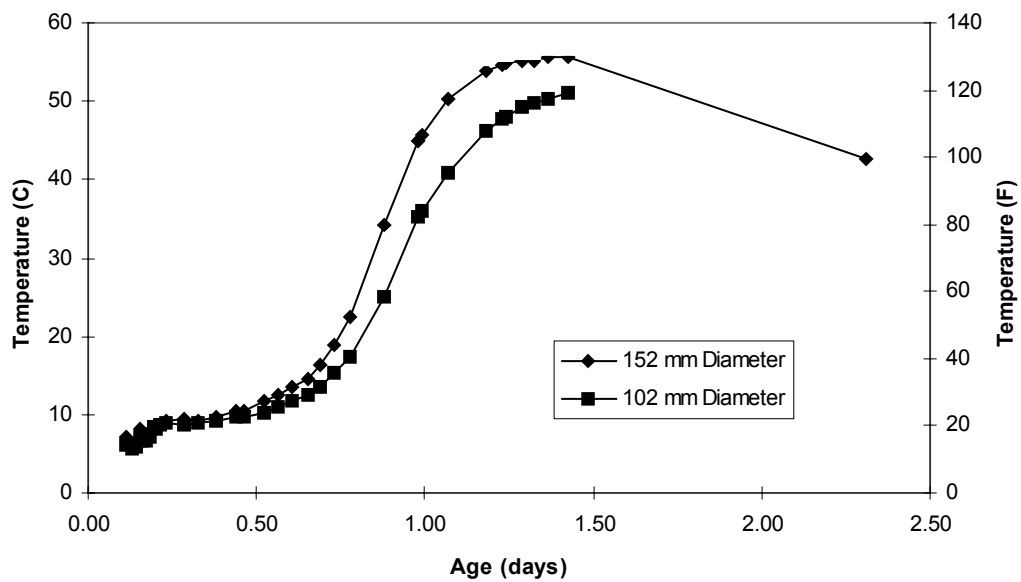


Figure 4.6. Hydration Temperature Histories of Girder 2C Cylinders

The compressive strength was measured for both the 152-mm and 102-mm (6-in and 4-in) diameter specimens just prior to loading, and the lower temperatures seem to have had a substantial effect. The strength of the 152-mm (6-in) diameter specimens was 63.4 MPa (9200 psi) compared with 46.9 MPa (6800 psi) in the 102-mm (4-in) diameter cylinders. These relate to stress-strength ratios of 0.43 and 0.59, respectively.

REFERENCES

- American Association of State Highway and Transportation Officials. *Standard Specifications for Highway Bridges*. 15th Edition. Washington, D. C., 1992.
- American Association of State Highway and Transportation Officials. *Standard Specifications for Highway Bridges*. 1st Edition LRFD. Washington, D. C., 1994.
- ACI Committee 209. "Prediction of Creep, Shrinkage, and Temperature Effects in Concrete Structures." *ACI Manual of Concrete Practice Part 1: Materials and General Properties of Concrete*. American Concrete Institute. Detroit, 1995.
- ACI Committee 318. *Building Code Requirements for Structural Concrete and Commentary*. American Concrete Institute. Farmington Hills, 1995.
- Barr, P., Fekete, E., Eberhard, M., Stanton, J, Khelaghi, B., and Hsieh, J. C. "High Performance Concrete in Washington State SR 18/ SR 516 Overcrossing." Washington State Department of Transportation Bridge and Structures Office. Olympia, Washington, 1998.
- Barr, Paul. *Behavior of High Performance Prestressed Concrete Girders*. Master's Thesis. University of Washington, 1997.
- Bazant, Zdenek P., and Yunping Xi. "Drying Creep of Concrete: Constitutive Model and New Experiments Separating its Mechanisms." *Materials and Structures*. Volume 27, 1994, pp.3-14.
- Branson, Dan E. *Deformation of Concrete Structures*. McGraw-Hill International Book Company. New York, 1977.
- Burns, N. H., and B. W. Russell. "Measured Transfer Lengths of 0.5 and 0.6 in Strands in Pretensioned Concrete Girders." *Prestressed Concrete Institute Journal*. Volume 41, No.5, September/October 1996, pp.44-63.
- Deatherage, H. J., and E. G. Burdette. "Development Length and Lateral Spacing Requirements of Prestressing Strand for Prestressed Concrete Bridge Girders." *Prestressed Concrete Institute Journal*. Volume 39, No.1, January/February 1994, pp.70-83.

Fekete, Elizabeth. "Prestress Losses in High Performance Concrete Girders". Master's Thesis. University of Washington, 1997.

Han, N., and J. C. Walraven. "Creep and Shrinkage of High-Strength Concrete at Early and Normal Ages." *Advances in Technology*. 1996, pp.73-94.

Neville, A. M. *Properties of Concrete*. Fourth Edition. Longman Group Limited. Essex, England, 1995.

Nilson, Arthur H. *Design of Prestressed Concrete*. Second Edition. John Wiley & Sons. New York, 1987.

Persson, Bertil. *Basic Deformations of High-Performance Concrete*. Nordic Concrete Research. Norsk Betonforening. Oslo, Norway, 1997.

Shahawy, M. A., M. Issa, and B. deV Batchelor. "Strand Transfer Lengths in Full Scale AASHTO Prestressed Concrete Girders." *Prestressed Concrete Institute Journal*. Volume 37, No.3, May/June 1992, pp.84-96.

Troxell, George Earl, Harmer E. Davis, and Joe W. Kelly. *Composition and Properties of Concrete*. McGraw-Hill Book Company. New York, 1968.

Sherman, M. R., and D. W. Pfeifer. "Testing of High-Performance Concrete According to AASHTO T 161, AASHTO T 277 and Modified AASHTO T 259 for Central Pre-Mix Prestress Co." WJE No. 962926, February 1998.